MAUSAM



DOI: https://doi.org/10.54302/mausam.v76i4.7112

Homepage: https://mausamjournal.imd.gov.in/index.php/MAUSAM

UDC No.551.583.16:551.577.37:551.524(540)

Future changes in extreme precipitation and warm days over megacities of India and the semi-arid Tirupati district

VENKATRAMANA KAAGITA^{1,2*}, VENUGOPAL THANDLAM^{3&,4,5}, VENKATRAMANA REDDY SAKIREVUPALLI^{1#}BYJU POOKKANDY^{2!} and BATHIREDDY GARI SAROJAMMA⁶

 $^{1}Department\ of\ Physics,\ Sri\ Venkateshwara\ University,\ Tirupati,\ India\ (^{\#}drsvreddy123@gmail.com).$ $^{2}The\ Energy\ and\ Resources\ Institute,\ New\ Delhi,\ India\ (^{!}Byjup_c@teri.res.in).$

³Air, Water and Landscape Science (LUVAL), Department of Earth Sciences, Uppsala University, Uppsala, Sweden (&venu.thandlam@geo.uu.se)

⁴Centre of Natural Hazards and Disaster Science, Uppsala University, Uppsala, Sweden ⁵The Centre for Environment and Development Studies Research Forum, Uppsala University, Uppsala, Sweden

⁶Department of Statistics, Sri Venkateshwara University, Tirupati, India (saroja14397@gmail.com) (Received 10 October 2024, Accepted 15April 2025)

*Corresponding author's email: K.Venkatramana007@gmail.com

सार— हम भारत के चुनिंदा महानगरों और अर्ध-शुष्क तिरुपति जिले में अत्यधिक वर्षा और उष्ण दिनों में भविष्य में होने वाले परिवर्तनों का अध्ययन करते हैं। यह कार्य जलवायु परिवर्तन जांच और सूचकांक (ETCCDI) पर विशेषज टीम के सूचकांकों का उपयोग करके जलवायु चरम सीमाओं में अनुमानित परिवर्तनों को संश्लेषित करता है। यह ऐतिहासिक[े] अविध के लिए आईएमडी से ग्रिडिंड वर्षा और तापमान डेटा और 2026-2100 के लिए मध्यम (SSP2-4.5) और उच्च (SSP5-8.5) वार्मिंग परिदृश्यों के तहत NEX-GDDP-CMIP6 डेटासेट से भविष्य के अनुमानों का उपयोग करता है। अनुमानों से पता चलता है कि विश्लेषित शहरों में औसत वार्षिक वर्षा और भारी वर्षा वार्ले दिनों की संख्या में लगातार वृद्धि हो रही है, जिसमें उच्च उत्सर्जन परिदृश्य के तहत बड़ी वृद्धि हुई है। लगातार गीले दिनों में परिवर्तन स्थानिक विविधता प्रदर्शित करते हैं तिरुपति जिले के लिए, दोनों ही परिदृश्यों में वार्षिक वर्षा में वृद्धि का अनुमान है, जिसमें दक्षिण-पश्चिम मॉनसुन के मौसम में विशेष रूप से उल्लेखनीय वृद्धि देखी जा रही है। तिरूपित में सभी मौसमों में पर्याप्त गर्मी का अनुमान[े]है, जिसमें मॉनसून-पूर्व मौसम में सबसे अधिक गर्मी पड़ने की उम्मीद है। ये निष्कर्ष क्षेत्र-विशिष्ट अनुकुलन रणनीतियों की महत्वपूर्ण आवश्यकता पर बल देते हैं और इस बात पर प्रकाश डालते हैं कि भविष्य के उत्सर्जन मार्गे जलवायु प्रभावों की गंभीरता को कैसे महत्वपूर्ण रूप से प्रभावित करेंगे। अनुमानों से पता चलता है कि विश्लेषित शहरों में औसत वार्षिक वर्षा और भारी वर्षा वालें दिनों की संख्या में लगातार ^वद्धि हो रही है, तथा उच्च उत्सर्जन परिदृश्य में यह वदधि और भी अधिक है। लगातार बारिश वाले दिनों में बदलाव स्थानिक विषमांगता को दर्शाते हैं. जो सभी शहरों में एक समान प्रवित्त के बिना जिटल पैटर्न प्रदर्शित करते हैं। सभी शहरों में एक ससंगत और तीव्र तापमान वृद्धि की प्रवृत्ति का अनुमान लगाया गया है, जिसके परिणामस्वरूप पूरी शताब्दी में, विशेष रूप से SSP5-8.5 परिदृश्य के तहत, गर्मे दिनों की आवृत्ति में उल्लेखनीय वृद्धि होगी। तिरुपति जिले के लिए, दोनों परिदृश्यों में वार्षिक वर्षा में वृद्धि होने का अनुमान है, जिसमें दक्षिण-पश्चिम मॉनसून के मौसम में विशेष रूप से उल्लेखनीय वृद्धि देखी जाएगी। तिरुपति में सभी मौसमों में पर्याप्त उष्णता का अनुमान है, और मॉनसून-पूर्व ऋत् में प्रचण्ड उष्णता की उम्मीद है। ये निष्कर्ष क्षेत्र-विशिष्ट अनुकूलन रणनीतियों की महत्वपूर्ण आवश्यकता पर बेल देतें हैं तथा इस बात पर प्रकाश डालते हैं कि भविष्य के उत्सर्जन मार्ग किस प्रकार जलवाय प्रभावों की गंभीरता को महत्वपूर्ण रूप से प्रभावित करेंगे।

ABSTRACT. We study future changes in extreme precipitation and warm days over selected megacities of India and the semi-arid Tirupati district. This work synthesises projected changes in climate extremes using indices from the Expert Team on Climate Change Detection and Indices (ETCCDI). It utilises gridded rainfall and temperature data from IMD for the historical period and future projections from the NEX-GDDP-CMIP6 dataset under moderate (SSP2-4.5) and high (SSP5-8.5) warming scenarios for 2026-2100. Projections indicate a consistent increase in both mean annual precipitation and the number of heavy rainfall days across the analysed cities, with larger increases under the high-emissions scenario. Changes in consecutive wet days exhibit spatial heterogeneity, displaying complex patterns without a uniform trend across all cities. A consistent and accelerating warming trend is projected across all cities, leading to a significant increase in warm-day frequency throughout the century, particularly under the SSP5-8.5 scenario. For the Tirupati district, annual precipitation is projected to increase under both scenarios, with the southwest monsoon season showing particularly notable enhancement. Substantial warming is also projected across all seasons for Tirupati, with the

pre-monsoon season expected to experience the most severe warming. These findings emphasise the critical need for tailored, region-specific adaptation strategies and highlight how future emissions pathways will significantly influence the severity of climate impacts.

Key words— Climate change, Extreme precipitation, Warm days, Indian megacities, Tirupati district, Climate indices.

1. Introduction

Climate change, driven predominantly anthropogenic activities such as fossil fuel combustion, deforestation, and industrial processes, has emerged as one of the most significant global challenges of the 21st century. The Earth's average surface temperature has risen by approximately 1.1 °C since the pre-industrial era, with profound implications for weather patterns, ecosystems, and human societies (IPCC, 2021). Among the most alarming consequences of global warming are the projected increases in the frequency, intensity, and duration of extreme weather events, including heat waves, heavy rainfall, droughts, and tropical cyclones, which pose severe risks to natural and human systems, particularly in vulnerable regions like India, where a large population depends on climate-sensitive sectors such as agriculture and water resources. The intensification of climate extremes is well-documented, with the Intergovernmental Panel on Climate Change (IPCC) Sixth Assessment Report (AR6) highlighting that humaninduced climate change has already increased the frequency and severity of extreme weather events globally, trends expected to worsen with further warming (IPCC, 2021).

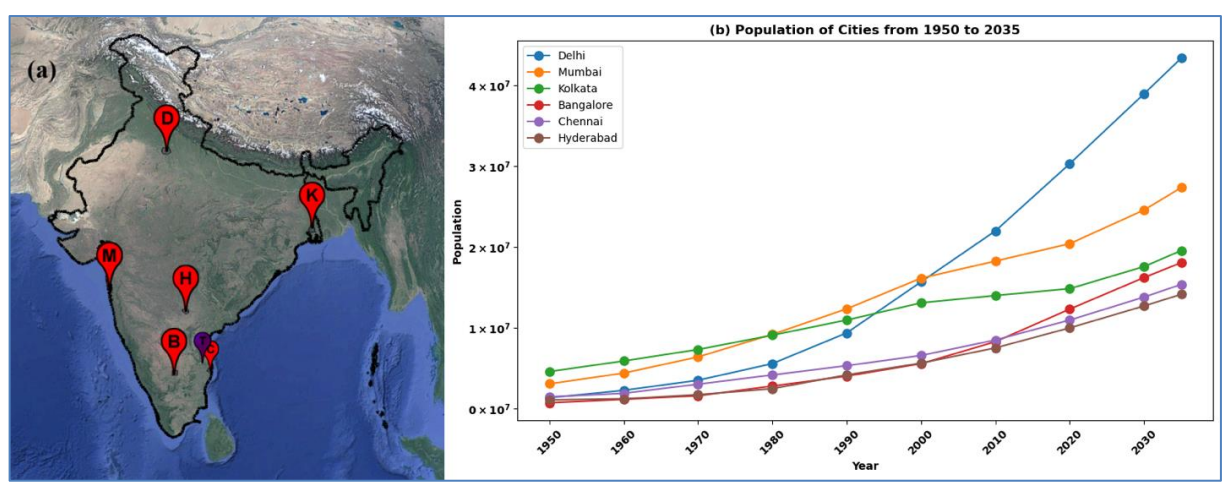
Over India, observational records and climate model projections indicate a significant rise in the intensity and duration of heatwaves, with some regions experiencing temperatures exceeding 45 °C for prolonged periods (Mishra et al., 2020). Concurrently, the frequency of heavy rainfall events has increased, particularly in central India, where a threefold rise in widespread extreme rain events has been observed since the mid-20th century (Roxy et al., 2017). These changes are attributed to the warming of the Indian Ocean, which enhances atmospheric moisture content and alters monsoon dynamics, leading to more intense precipitation events (Krishnan et al., 2020). Additionally, the frequency of extreme rainfall events is strongly influenced by climate phenomena such as the El Niño-Southern Oscillation (Trenberth, 1997; Ashok et al., 2004; McPhaden et al., 2006; Hrudyam et al 2021), Madden-Julian Oscillation (Zhang, et al., 2005; Vitart, et al., 2017), Pacific Decadal Oscillation (Mantua et al., 1997; Newman et al., 2016), Quasi-Biennial Oscillation (Baldwin et al., 2001; Anstey & Shepherd, 2014), Atlantic Multidecadal Oscillation (Enfield et al., 2001; Knight et al., 2006), and the Indian Ocean Dipole (Sajiet al., 1999; Webster et al., 1999), which also modulate the intensity of the Indian summer

monsoon (Gadgil, 2003; Nishimoto and Yoden, 2017; Wang et al., 2001).

1.1. Regional climate change across India

India's diverse climate, influenced by its vast geographical expanse, results in varying impacts of climate change across the country. The Himalayan region, including states like Jammu and Kashmir and Uttarakhand, is experiencing accelerated glacier retreat and increased extreme rainfall events due to global warming, threatening water security and causing devastating floods and landslides (Shrestha et al., 2012; Bolch et al., 2012; Allen et al., 2016; Krishnan et al., 2019). The Indo-Gangetic Plains, which are crucial for agriculture, face rising temperatures and water stress, with heatwaves and extreme rainfall events posing risks to food security and rural livelihoods (Mishra et al., 2020; Yaduvanshi et al., 2021; Roxy et al., 2017; Rao et al 2023). Western India, with its arid climate, is vulnerable to droughts and desertification, while coastal areas face sea-level rise and cyclonic activity (Mujumdar et al., 2020; Dash et al., 2012; Singh et al., 2014; Mahapatra et al, 2015; Dai et al., 2017). Southern India experiences variability in rainfall, characterised by declining monsoon rains and an increase in extreme events, which threaten agriculture and infrastructure (Mujumdar et al., 2020; Mishra and Shah, 2018; Mohanty et al., 2020; Rao et al., 2020; Ramesh et al., 2015).

Eastern India, particularly states like West Bengal and Odisha, is highly susceptible to cyclones and flooding, with the Bay of Bengal being a cyclone hotspot (Mohanty et al., 2020; Rao et al., 2020; Mirza, 2002). The region faces severe impacts on agriculture, fisheries, human settlements. India's extensive coastline, spanning over 11,000 km, is vulnerable to sea-level rise, leading to coastal erosion and saltwater intrusion, particularly in low-lying areas such as the Sundarbans (Hazra et al., 2002). Cities along the coast, including Mumbai, Chennai, and Kolkata, are likely to experience increased flooding and structural damage to infrastructure such as roads and buildings due to heavy rainfall and storm surges (Krishnan et al., 2020). The livelihoods of millions who depend on fishing and coastal agriculture are threatened, underscoring the need for urgent adaptation measures. These regional disparities highlight the need for tailored adaptation strategies to address the distinct challenges posed by climate extremes across India.



Figs. 1(a&b). (a) Geographical locations of the megacities selected in the study represented with the first letters in their names. (b) Population growth across megacities from 1950 to 2035

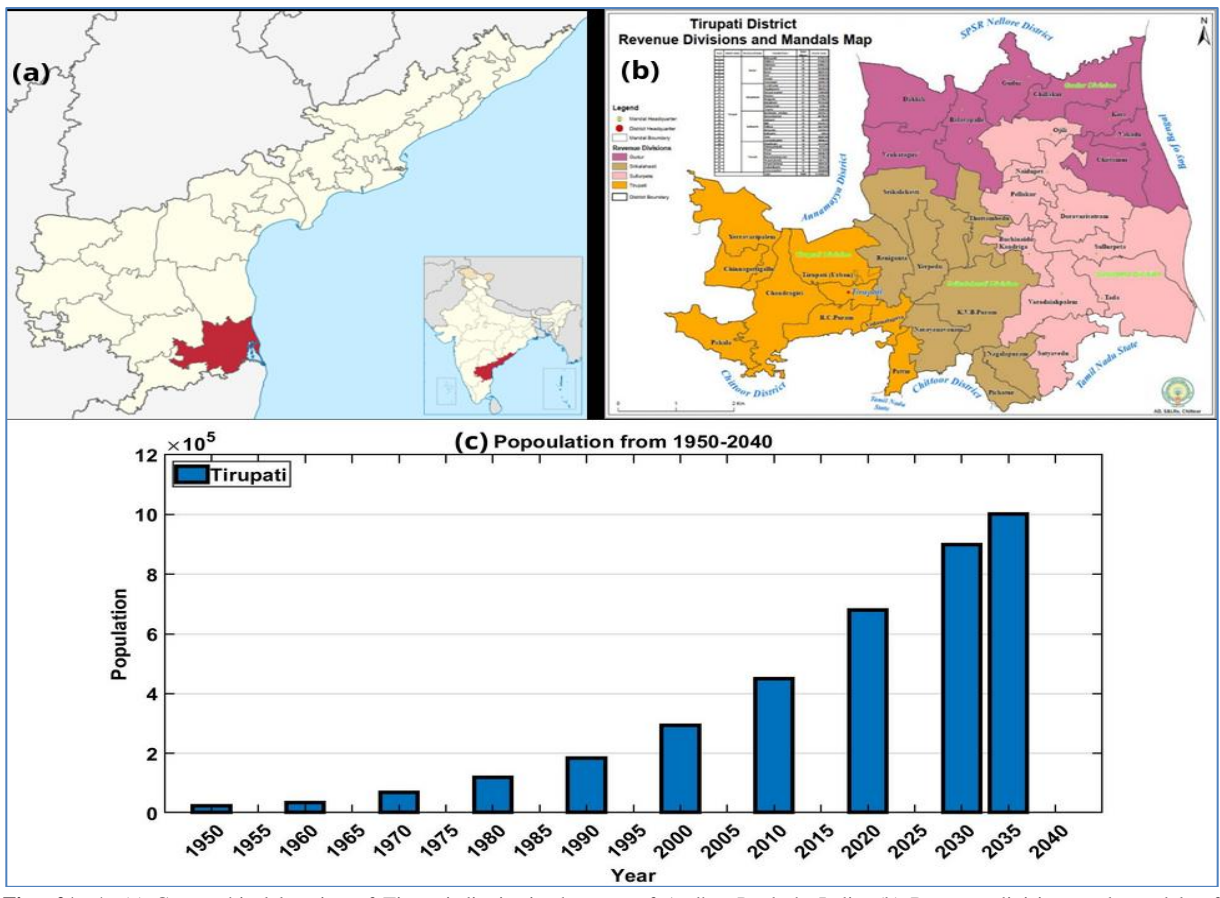
1.2. Socio-economic impacts and adaptation challenges

The socio-economic impacts of changing climate extremes in India are profound and multifaceted. Agriculture, which employs nearly 50% of the population and contributes significantly to the national economy, is susceptible to variations in temperature and precipitation. Increased heatwaves and erratic rainfall patterns can lead to crop failures, reduced yields, and food insecurity, particularly for staple crops like wheat and rice (Yaduvanshi et al., 2021). For instance, a study by Lobell et al. (2012) found that wheat yields in India could decline by 6-23% by 2050 due to rising temperatures. Urban areas, which are home to over 34% of India's population, are also at risk, with megacities such as Mumbai, Delhi, and Chennai facing heightened vulnerabilities to urban flooding, heat stress, and waterlogging (Revi et al., 2014). The 2015 Chennai floods and the 2018 Kerala floods serve as stark reminders of the devastating impacts of extreme rainfall on infrastructure, livelihoods, and public health (Mishra and Shah, 2018).

Furthermore, marginalised communities, including smallholder farmers, informal sector workers, and low-income urban dwellers, are disproportionately affected by these extremes, exacerbating existing inequalities and highlighting the need for equitable climate adaptation policies (O'Brien et al., 2004; Hallegatte et al., 2016; Rohini et al, 2019). As India grapples with the dual challenges of climate change and socio-economic development, a deeper understanding of projected climate extremes is essential for safeguarding vulnerable populations and ecosystems in the face of an uncertain future. Therefore, understanding regional and local climate change is critical for developing effective grassroots mitigation, adaptation, and resilience strategies.

This paper aims to synthesise projected changes in climate extremes over urban India, focusing on key climate indices derived from the joint CCI/WCRP-Clivar/JCOMM Expert Team on Climate Change Detection and Indices (ETCCDI). The study examines future changes in indices such as consecutive wet days, heavy precipitation days, and warm days across six major cities spanning different parts of India (Fig. 1a). This is particularly important, as the population growth in megacities (Fig. 1b) is evident from 1950 to 2035. Delhi has experienced the most dramatic growth, surpassing Mumbai around 2000 to become India's most populous city and is projected to reach over 40 million inhabitants by 2035. All cities exhibit steady population increases over this period, with Delhi and Mumbai displaying the steepest growth curves, while Chennai and Hyderabad have more moderate growth trajectories, remaining below 20 million through 2035 (Fig. 1b).

This study aims to contribute to India's growing understanding of climate change impacts by examining regional variations, socio-economic implications, and the underlying mechanisms driving these changes. Hence, the work also focused on a major pilgrimage site, the historical and rapidly developing district of Tirupati, located in a semi-arid region of southeastern India (Fig. 2). Tirupati, a rapidly developing district located between 13° and 14° N and 79° and 80° E, is bordered by the Bay of Bengal to the east and the state of Tamil Nadu to the south. With an area of 9174 square km, it accounts for 5.63% of the state's total area and has over 3 million inhabitants. The mountainous region has an elevation of 2500 feet above sea level. Chennai and Bangalore are located 150 km south and 250 km west of Tirupati, respectively. The district is known for its groundnut, paddy, red sandalwood, sugarcane, and other olericulture,



Figs. 2(a-c). (a) Geographical location of Tirupati district in the state of Andhra Pradesh, India. (b) Revenue divisions and mandals of Tirupati district. (c) Population growth in the city of Tirupati during 1950-2035

pomology, and floriculture products. The Eastern Ghats dominate the western and northern region, gradually bending towards the sacred hills of Tirupati, passing through Chandragiri and entering the Nellore district.

Tirupati, the southernmost major city in Andhra Pradesh, is a smart city recognised for its strengths in education, IT, telecommunications, mobile services, banking, real estate, and healthcare sectors. It attracts over a million people daily for employment, education, healthcare, welfare, travel, and development. The city's international airport and well-connected transportation system facilitate travel. Tirupati is famous for the Lord Venkateshwara temple, also known as Balaji, which attracts 60,000-80,000 daily visitors, making it one of the world's richest Hindu temples. This pilgrimage contributes to the city's economy, with an average annual revenue of USD 529.27 million. The district also features sacred places, such as the Srikalahasti temple, and boasts a coastline along the Bay of Bengal. Sriharikota, India's primary rocket/satellite launch site, is located in the district. Thus, rapid urbanisation and increased visitation have led to environmental challenges, including service

stress, pollution, and resource degradation. Thandlam *et al.* (2024) elaborate on Tirupati's significance. Figs. 2(a &b), accessed from the Andhra Pradesh State government website on January 2, 2025 (https://tirupati.ap.gov.in/map-of-district/), show the district's shape.

Fig. 2(c) shows Tirupati's population growth from 1950 to 2035 (World-PopulationReview.com). Starting with a tiny population in 1950 (less than 100,000 residents), Tirupati city has experienced consistent growth over the decades. The growth accelerated notably after 1990, showing a steeper upward trajectory. By 2020, the population reached approximately 700,000, projections suggest it will exceed 1 million by 2035. This represents a more than tenfold increase over the 90 years, Tirupati's significant urbanisation and development as an important regional centre in southern India. Hence, understanding future climate change and extreme climate indices over the district is crucial for planning, management, and mitigation.

This paper is organised as follows: Section 2 describes the data and methods used in the work. Section

TABLE 1
Definitions of different indices used in this study

S. no	Indices	Definition
1.	Consecutive wet days	Count the number of spells that are ≥ 1 mm.
2.	Heavy precipitation days	Count the days on which rainfall $> 90^{\text{th}}$ percentile value of the reference period.
3.	Warm days	Count the days on which the maximum temperature > 90 th percentile value of the reference period.

3 shows future changes in rainfall, T_{max} and T_{min} , along with future projections of climate indices across different cities and the Tirupati district. We summarise and conclude the paper in Section 4.

2. Data and methodology

This study utilises daily gridded rainfall data from the Indian Meteorological Department (IMD) with a spatial resolution of 0.25 $^{\circ}$ x 0.25 $^{\circ}$ from 1981 to 2010 as a reference. This data was used to evaluate the historical climate conditions over India and the Tirupati district. Extreme values were determined based on the 90th percentile of the dataset covering the period from 1981 to 2010. Following the IMD annual report, the reference period of 1981-2010 (as reported in the IMD annual report 2022) was used to compute these indices. Future studies will utilise data from the latest Coupled Model Intercomparison Project Phase 6 (CMIP6) models in different scenarios. The NEX-GDDP-CMIP6 dataset comprises global downscaled climate scenarios derived from the General Circulation Model (GCM) runs conducted as part of the CMIP6 (Eyring et al., 2016).

The climate indices were computed using scientifically valid definitions from the Expert Team on Climate Change Detection and Indices (ETCCDI) (Table 1) (Chaubey et al., 2022; Zhang et al., 2011). To gain a uniform perspective on observed changes in weather and climate extremes, ETCCDI has defined a core set of descriptive indices of extremes. The indices describe particular characteristics of extremes, including frequency, amplitude and persistence. The core set includes 27 extreme indices for temperature and precipitation. Thandlam et al. (2024) studied 7 climate indices over Tirupati and found that the extreme indices shown in Table 1 show the most prominent changes in the recent decades over Tirupati. Additionally, the selected index is relevant to health, agriculture, food security, water resources, disaster risk reduction, and energy sectors.

The GCMs used in this study were statistically downscaled to a resolution of 0.25 $^{\circ}$ × 0.25 $^{\circ}$ and bias-

corrected for daily time scales (Eyring et al., 2016). The parameters analysed included daily rainfall, maximum temperature (T_{max}) , and minimum temperature (T_{min}) . The study assessed two warming scenarios: a high warming scenario (SSP5-8.5; representing a high emissions/fossilfueled development pathway) and a medium warming scenario (SSP2-4.5; representing emissions/stabilisation pathway). To minimise uncertainty in models, the ensemble mean from 29 models (shown in Table S1) was utilised for both historical data (1981-2010) and future projections (2026-2100). The ensemble from 29 models is calculated by first bringing all model outputs to a common basis (e.g., the same spatial grid and time period) and then averaging their values. At each grid point and time step, the arithmetic mean is taken across all models, so that the contribution from each model is equal. This averaging smooths out model-specific biases and random noise, providing a more robust estimate of the climate signal than any single model alone. The future periods were categorised into three epochs: near future (NF, 2026-2050), mid-future (MF, 2051-2075), and far future (FF, 2076-2100).

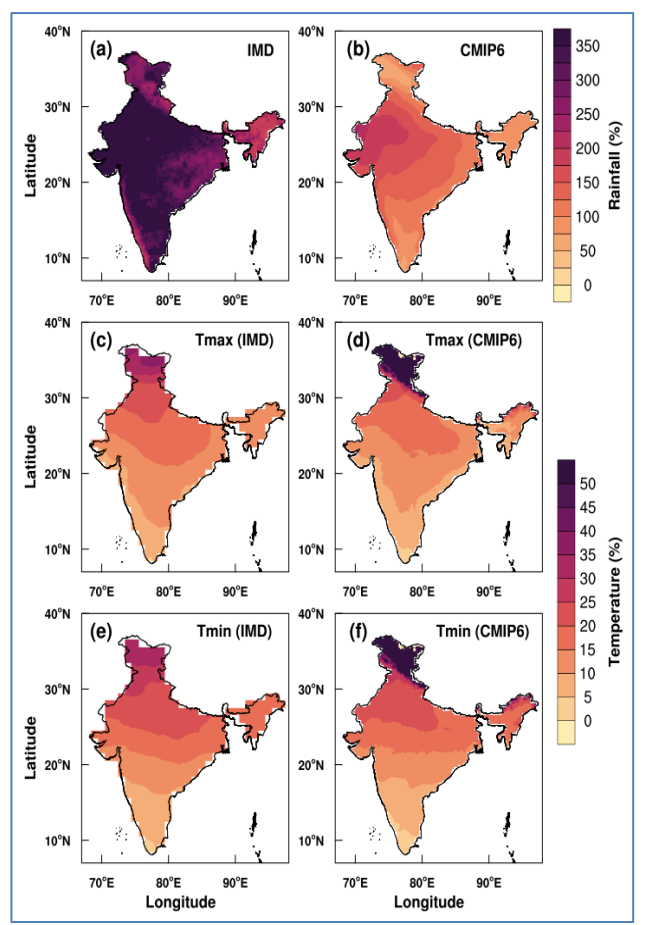
3. Results and discussion

Fig. 3 illustrates the spatial variability of three climatic variables-rainfall, T_{max} , and T_{min} across India, using the Coefficient of Variation (CV) as a measure. In the historical period (1981-2010; Figs. 3(a-f), observed IMD data and CMIP6-based simulations both reveal a pronounced coast-to-interior gradient in monsoon rainfall variability when measured by the CV as shown in equation 1. Along the windward Western Ghats and in northeastern India, where mean seasonal totals exceed 2,500 mm, the CV is lowest ($\approx 25-50$ %), reflecting the damping effect of high mean rainfall. Moving inland across the Deccan Plateau and central India, CV values rise to moderate levels ($\approx 75-125$ %), before peaking at > 150-200 % in the rain-shadow of the Ghats and across northwestern India, where low mean totals amplify relative interannual swings. While CMIP6 broadly captures this north-south gradient, it systematically underestimates variability over central India by 10-20 % and overestimates CV by up to 30 % in parts of the northeastern foothills (Turner and Annamalai, 2012).

Coefficient of variation (%) =
$$(\sigma/\mu) \times 100$$
 (1)

 σ = standard deviation of the climate variable μ =mean of the climate variable

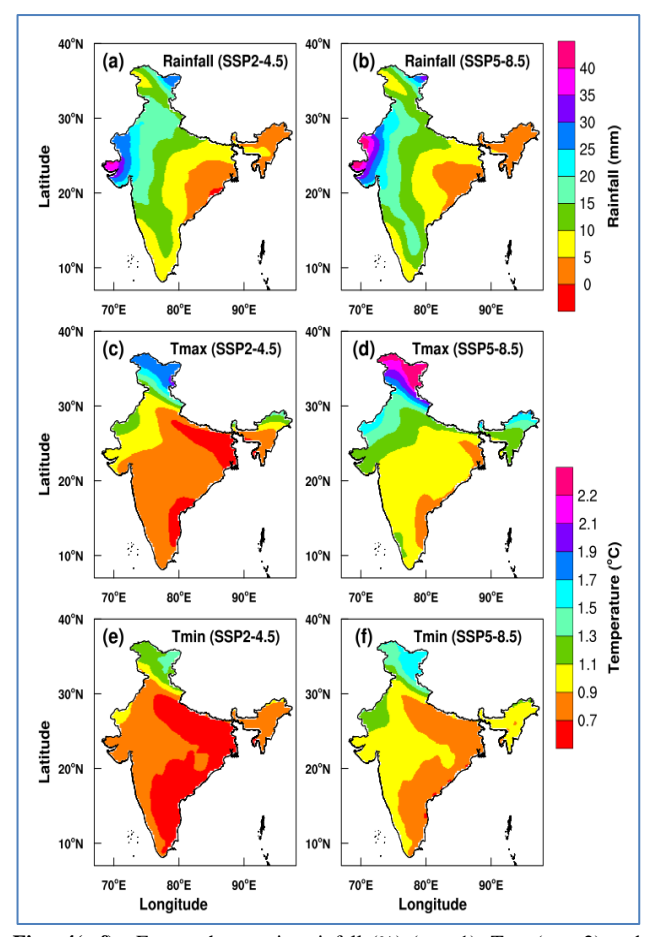
Temperature variability exhibits a similarly coherent spatial structure. Both T_{max} and T_{min} CV increase steadily from the southern peninsular regions toward the high elevations of the Himalaya. In peninsular India, maritime



Figs. 3(a-f). Coefficient of variability (%) for precipitation (row 1), T_{max} (row 2) and T_{min} (row 3). Column 1 for IMD and column 2 for CMIP6 ensemble

buffering keeps the CV low (<5% for T_{max} ; <3% for T_{min}), whereas the Himalayan foothills and northwest India record high thermal CV (>15% for T_{max} ; >10% for T_{min}). CMIP6 reproduces these gradients with only minor biases (e.g., a modest underestimation of T_{max} CV by $\sim2\%$ over the Indo-Gangetic Plain).

Looking ahead to 2021-2050 Figs. 4(a-f), CMIP6 projections under SSP2-4.5 and SSP5-8.5 indicate that the most pronounced increases in seasonal precipitation ($\Delta P \approx 20\text{-}40 \text{ mm}$) remain concentrated along the west coast and Himalayan foothills areas that historically exhibit low relative variability but high absolute rainfall totals. Conversely, central India and the Ghats' rain-shadow, despite their high historical CV, experience only moderate wetting ($\Delta P \approx 10\text{-}20 \text{ mm}$). Under the high-emissions SSP5-8.5 scenario, these precipitation gains are amplified by an additional 5-10 mm compared to SSP2-4.5. These results deviate from earlier CMIP5 assessments, which suggested a closer linkage between historical variability hotspots and future wetting intensity (Turner and Annamalai, 2012).

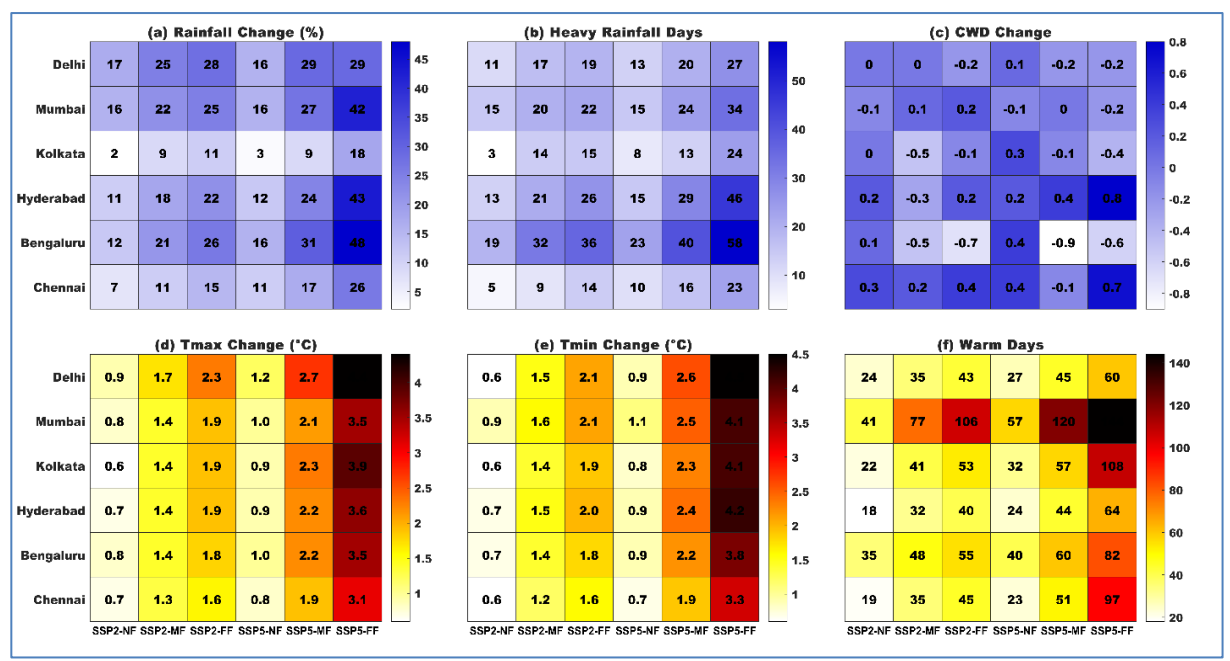


Figs. 4(a-f). Future changes in rainfall (%) (row 1), T_{max} (row 2) and T_{min} (row 3). Column 1 for SSP2-4.5 and column 2 for SSP5-8.5

Projected temperature changes further underscore elevation-dependent amplification. Warming in T_{max} is greatest in the northwest and Himalayan regions, with ΔT_{max} of ~2.0-2.5 °C under SSP2-4.5 and up to ~4.0 °C under SSP5-8.5. In contrast, peninsular and coastal regions warm by less than 1.5 °C under the moderate-emissions pathway. $T_{\text{min}} \\$ increases uniformly across more the subcontinent $(\Delta T_{min} \approx 1.0\text{-}1.5 \,^{\circ}\text{C})$ under SSP2-4.5; 1.5-2.2 $^{\circ}\text{C}$ under SSP5-8.5), resulting in a narrowing of the diurnal temperature range, a hallmark of nighttime warming amplification (Rangwala and Miller, 2012; Seneviratne et al., 2016).

3.1. Future absolute changes in precipitation and wet days over megacities

A consistent projection across all analysed cities is an increase in both mean annual precipitation (as a percentage) (Fig. 5a) and the change in the number of heavy rainfall days (Fig. 5b) per year under both SSP scenarios throughout the 21st century. This dual increase



Figs. 5(a-f). The projected changes in (a) rainfall (%), (b) annual heavy rainfall days, (c) consecutive wet days, (d) maximum temperature (T_{max}) , (e) minimum temperature (T_{min}) , and (f) the number of warm days across different cities for the near future (NF), mid future (MF), and far future (FF) under the SSP2-4.5 and SSP5-8.5 scenarios

points not only to wetter conditions on average but also to a substantially more frequent occurrence of intense rainfall events. These findings align with broader climate model projections indicating an intensification of the hydrological cycle and the South Asian monsoon under future warming, often characterised by increases in both mean and extreme precipitation frequency and intensity (IPCC, 2021; Mishra et al., 2020; Ali et al., 2021). For both metrics, the magnitude of the projected increase generally amplifies over time (NF < MF < FF) and is significantly larger under the high-emissions SSP5-8.5 scenario compared to the moderate SSP2-4.5 scenario. This divergence between scenarios becomes particularly stark in the future, emphasising the strong control of future emissions pathways on average rainfall and the frequency of extreme events (Dubey et al., 2021; IPCC, 2021).

Considerable spatial heterogeneity is evident for both mean and extreme precipitation changes. Bengaluru consistently shows the highest projected increases, with mean rainfall increasing by up to 48% and the number of heavy rainfall days increasing by up to 58 days per year under SSP5-8.5 in the FF. Hyderabad also projects substantial increases, with mean rainfall rising by up to 42% and the number of heavy rainfall days increasing by up to 46 days per year (SSP5-8.5 FF). Mumbai experiences significant increases in both mean rainfall (up to 41%) and the number of heavy rainfall days (up to 34 days/year). Delhi also experiences

considerable increases. Conversely, Kolkata exhibits the most modest increases in both metrics (*e.g.*, up to 18% mean increase and up to 24 additional heavy rainfall days per year under SSP5-8.5 FF), while Chennai displays moderate increases relative to cities like Bengaluru or Hyderabad. These regional variations highlight the impact of local and regional climatic factors on the broader climate change signal (Mujumdar *et al.*, 2020; Mathison *et al.*, 2015).

Fig. 5(c) illustrates the projected absolute change in consecutive wet days per year for six major Indian cities. The projected changes in wet days present a complex and spatially heterogeneous picture, markedly different from the consistent increases observed for mean precipitation and heavy rainfall frequency in the same cities. There is no uniform trend of increase or decrease across all locations, scenarios, or time periods. Hyderabad and Chennai generally project slight increases in the maximum length of wet spells, particularly under SSP5-8.5 in the FF (increases of 0.8 and 0.7 days, respectively). In contrast, Bengaluru and Kolkata tend towards decreases in wet days, especially in the MF-to-FF under both scenarios. For instance, Bengaluru projects decreased by 0.5 to 0.9 days, while Kolkata showed a reduction of up to 0.5 days. Delhi and Mumbai exhibit minimal changes, typically small decreases (-0.1 to -0.2 days) in the later periods.

Unlike rainfall amount or intensity indices, changes in the number of wet days do not show a clear

amplification over time across all cities. Similarly, the high-emission SSP5-8.5 scenario does not consistently produce larger changes (either positive or negative) compared to SSP2-4.5 for all locations. Despite projected increases in total rainfall and heavy rain events, the lack of a consistent increase in wet days suggests potential shifts in precipitation patterns. The findings suggest that future rainfall, although potentially heavier on average and featuring more intense events, may not necessarily occur in longer, continuous spells in all regions. In cities like Bengaluru and Kolkata, the projected increase in rainfall intensity may be accompanied by shorter wet periods or longer intervening dry spells, resulting in a decrease in consecutive wet days (IPCC, 2021; Sillmann et al., 2013). This highlights that changes in different aspects of the precipitation regime (mean, intensity, duration, frequency) do not always scale uniformly and can exhibit divergent trends depending on regional dynamics (Pfahl et al., 2017). However, the projected increases in wet days in Hyderabad and Chennai suggest that longer wet spells might accompany the overall increase in rainfall in these locations.

The projected changes in annual "warm-day" frequency and surface temperatures across six major Indian metropolises reveal a consistent and accelerating warming trend through the twenty-first century, particularly under the high emissions SSP5-8.5 scenario. As shown in Fig. 5f, even under the moderate emissions pathway (SSP2-4.5), warm-day counts rise from the NF baseline (2026-2050) by roughly 18-41 days/year to 35-77 days/year in the MF(2051-2075) and 40-106 days/year by the FF (2076-2100). Under SSP5-8.5, these increases are 10-20 days greater in mid-century and surge by an additional 40-60 days by late century, culminating in Mumbai experiencing nearly 144 extra warm days per year, effectively subjecting its population to extreme-heat conditions on almost 40% of all days annually (IPCC, 2021).

Delhi, while not topping the warm-day tally, exhibits the most pronounced rise in daytime T_{max} : from +0.9 °C (SSP2-4.5, NF) to +2.3 °C (SSP2-4.5, FF), and under SSP5-8.5 soaring to +4.4 °C by 2100 (Fig. 5d). Mumbai and Kolkata follow closely, with T_{max} increases of +3.5 °C and +3.9 °C, respectively, under SSP5-8.5 FF. These magnitudes align with regional downscaling studies of CORDEX South Asia, which forecast urban-scale warming of 3-5°C in densely built areas absent significant mitigation (Mishra *et al.*, 2020). Notably, under SSP5-8.5, the mid-future jump in T_{max} (\approx +2.1 to +2.7°C across cities) exceeds the total end-of-century rise under SSP2-4.5, underscoring the critical importance of near-term emissions pathways for limiting mid-century heat stress. Nighttime T_{min} increases at least as rapidly as daytime

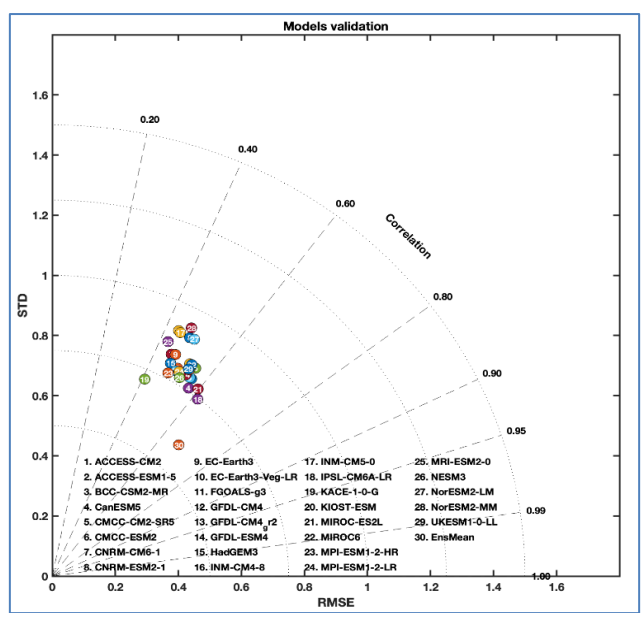


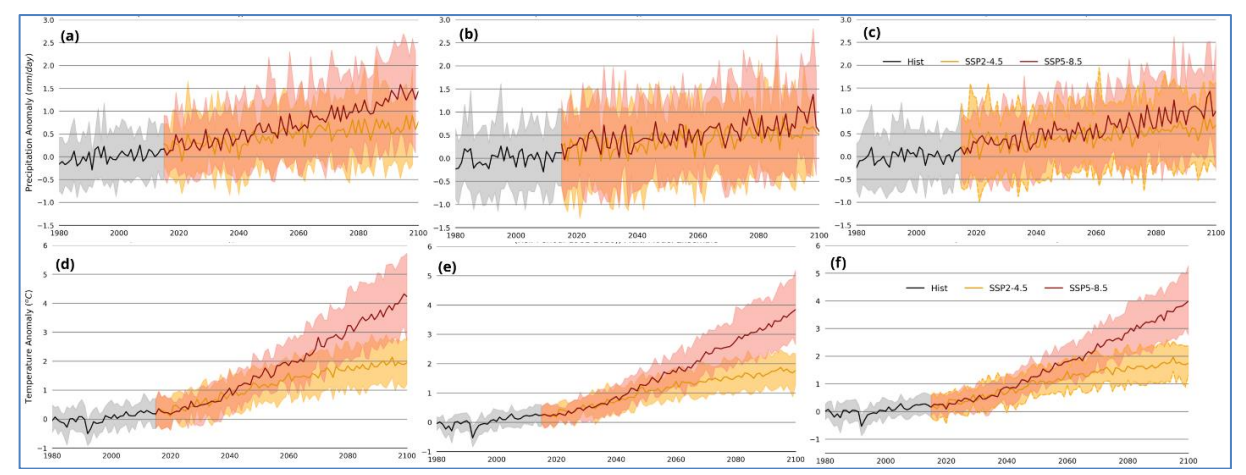
Fig. 6. IMD (vs) CMIP6 models over Tirupati district during 1981-2010 reference periods

highs Fig. 5(e). Under SSP5-8.5 FF, T_{min} gains range from +3.3 °C in Chennai to +4.5 °C in Delhi, compared with SSP2-4.5 FF projections of +1.6 °C to +2.1 °C. The disproportionate warming of nocturnal minima narrows the diurnal temperature range, hindering physiological recovery from daytime heat and exacerbating chronic heat-stress risks in vulnerable urban populations (Ali *et al.*, 2021). Prior work in Indian coastal cities has linked elevated nighttime temperatures to spikes in heat-related morbidity and mortality, particularly during multi-day heatwaves when nocturnal cooling is compromised, undermining human thermoregulation.

Inter-city contrasts highlight both geography and baseline climatology in shaping future heat burdens. Mumbai's monsoonal buffering affords a smaller absolute ΔT_{max} (+3.5°C) than Delhi (+4.4°C), yet its coastal humidity amplifies perceived heat stress when combined with 144 extra warm days under SSP5-8.5 FF (Dubey *et al.*, 2021). Kolkata and Chennai exhibit similar sensitivities, while inland hubs like Hyderabad and Bengaluru, although somewhat spared in warm-day counts, still face 60-82 additional hot days and +3.6 to +3.8°C of warming under high emissions. These differentials underscore the need for tailored adaptation strategies that consider local climatology, urban morphology, and socio-demographic vulnerability.

3.2. Climate models' skill over the semi-arid Tirupati district

The Taylor diagram (Fig. 6) illustrates the performance of 29 CMIP6 models and their ensemble



Figs. 7(a-f). (a) Projected changes in precipitation anomaly and (d) temperature anomaly over Bengaluru; (b) and (e) same as (a) and (d) but for Chennai; (c) and (f) same as (a) and (d) but for Tirupati

mean in simulating rainfall in the Tirupati district, compared to the IMD dataset, during the period 1981-2010. The analysis reveals considerable variation in model skill and highlights systematic tendencies common across many models. Most models demonstrate a reasonably high degree of pattern correlation (R values typically between 0.4 and 0.65) with the observed IMD rainfall, suggesting they capture the phasing of (e.g., seasonal or interannual) rainfall variations relatively well. The capability of CMIP6 models to represent large-scale precipitation patterns over regions such as South Asia, albeit with varying degrees of accuracy, has been documented in several evaluation studies (e.g., Gusain et al., 2020; Almazroui et al., 2020). However, a prevalent characteristic among most models is the underestimation of rainfall variability, as indicated by standard deviations that are generally lower than those of the IMD reference data. This suggests the models may fail to capture the full amplitude of observed rainfall fluctuations. Such underestimation of precipitation variability, particularly concerning daily or intraseasonal timescales, remains a persistent challenge in global climate models, including the CMIP6 generation (Gusainet al., 2020; Kim et al., 2020).

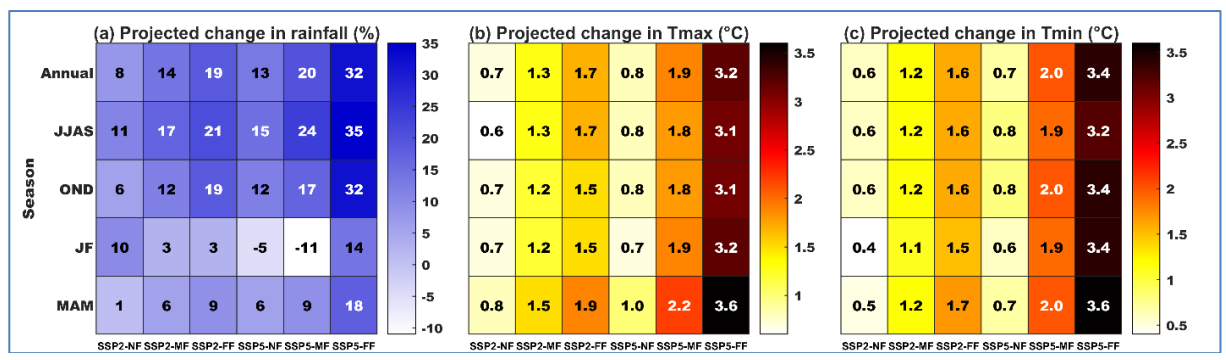
Specific models exhibit superior performance when overall skill is measured by the root mean square error (RMSE). Notably, MIROC-ES2L (21), INM-CM4-8 (15), and INM-CM5-0 (16) are positioned closest to the reference point, indicating a better balance between pattern correlation and amplitude representation compared to other models like FGOALS-g3 (11) or GFDL-CM4_gr2 (12), which show larger RMSE values. The significant inter-model spread in performance metrics is a typical feature of the CMIP6 ensemble, reflecting differences in model physics, parameterisations, and

resolution (Raghavan *et al.*, 2020; Eyring *et al.*, 2016). Furthermore, the multi-model ensemble mean (EnsMean, 30) demonstrates commendable skill, achieving a high correlation coefficient (~0.8) and a lower RMSE than many individual models. While it also slightly underestimates variability, its position near the reference point underscores the value of ensemble averaging. Multi-model ensembles often yield improvements in skill scores and provide more robust climate information than individual models by averaging specific model biases and internal variability noise (Tebaldi and Knutti, 2007; IPCC, 2021).

In conclusion, while CMIP6 models generally capture the pattern of Tirupati regional rainfall, accurately simulating its variability amplitude remains a challenge for most. Specific models (MIROC-ES2L, INM-CM4-8, INM-CM5-0) and the multi-model ensemble mean show higher overall fidelity to the IMD observations for this metric, highlighting the importance of considering model spread and the benefits of ensemble approaches in climate impact assessments. Better correlations and lower RMSE are expected in T_{max} and T_{min} over (not shown). Similarly, the CMIP6 data is expected to resemble the performance over other cities (not shown here). The performance of individual models over Tirupati is shown Supplementary Table S2.

3.3. Future climate change over the semi-arid Tirupati district

All three cities show a general increasing trend in precipitation anomalies throughout the projection period (2020-2100), though with notable differences in magnitude and variability. Tirupati (7c) exhibits significant projected precipitation variability, with peaks



Figs. 8(a-c). (a) Projected change in rainfall (%), (b) T_{max} (°C), (c) T_{min} (°C) in different future time periods for both SSPs and for different seasons over Tirupati district

exceeding 2 mm/day under the SSP5-8.5 scenario by 2100. The historical baseline shows moderate fluctuations, but future projections indicate more pronounced wet periods. Chennai (Fig. 7b) demonstrates substantial interannual variability in precipitation patterns. This aligns with observations by Prakash et al. (2015), who documented significant variability in rainfall datasets over South India, particularly in coastal regions such as Chennai, during the monsoon season. Bengaluru (Fig. 7a) exhibits a more gradual increase in precipitation anomalies compared to Chennai and Tirupati, with historical data indicating lower variability but future projections suggesting increased precipitation under highemission scenarios. These projections reflect the regional climate variability documented by Ramachandran et al. (2017), who observed significant temporal changes in precipitation patterns across Tamil Nadu, which are attributable to both natural and anthropogenic climate change factors.

Temperature anomalies show clear warming trends across all three cities, with important distinctions. Tirupati (Fig. 7f) exhibits the most pronounced temperature increase under SSP5-8.5, reaching 4 °C above baseline by 2100. Even under the moderate SSP2-4.5 scenario, warming exceeds 2 °C by the end of the century. Chennai (Fig. 7e) exhibits a warming pattern similar to Bengaluru, but with slightly lower variability, likely due to its coastal location. Srinivasan and Sibi (2021) identified urban heat island effects already impacting Chennai's metropolitan area, which may compound the projected climate warming trends. Bengaluru (Fig. 7d) exhibits a consistent warming trend, with temperature anomalies projected to reach approximately 4 °C under SSP5-8.5 and 2 °C under SSP2-4.5 by 2100. Singh et al. (2023) have already documented differential heat exposure across Bengaluru's urban landscape, with particularly concerning impacts on vulnerable populations. These warming projections are consistent with the broader findings of Mishra et al. (2017), who projected significantly increased heat wave exposure across India under 1.5 °C and 2 °C global

warming scenarios, with inland urban areas particularly vulnerable.

Comparing the three cities reveals essential differences in climate vulnerability. Tirupati appears vulnerable to both temperature and precipitation extremes, exhibiting high variability in rainfall patterns alongside substantial warming. As a significant religious & cultural centre in Andhra Pradesh, these climate changes could affect tourism and regional economic activities. As a major coastal metropolis, Chennai faces moderate temperature increases but significant variability in precipitation. Kothawale et al. (2016) documented longterm temperature trends that reveal warming signals across major Indian cities, with coastal cities such as Chennai exhibiting distinct patterns of change driven by both global and local factors. Bengaluru, while displaying substantial warming, shows more moderate changes in precipitation. The city's elevated plateau location and its surrounding forest ecosystems, which provide climate regulation services as documented by Dhanya and Ramachandra (2016), may influence its unique climate profile.

Fig. 8 presents comprehensive climate projections for the Tirupati district across multiple temporal horizons, i.e., NF, MF, and FF. The projections are displayed for the moderate SSP2 and the high-emission SSP5 scenario. The figure illustrates seasonal and annual changes in precipitation (Fig. 8a, expressed as %) and temperature parameters (T_{max} in panel 8b and T_{min} in Fig. 8(c), both described in °C). Fig. 8(a) reveals a consistent trend of increasing annual precipitation across all periods under both scenarios, with particularly notable findings. The most substantial precipitation increases are projected for the FF under the SSP5 scenario, with annual precipitation expected to increase by 32%. Seasonal analysis reveals that the southwest monsoon period (JJAS) experienced the most significant precipitation enhancement, with a 35% increase in the FF under SSP5-8.5. The post-monsoon season (OND) also shows significant precipitation

increases, particularly under SSP5-8.5 FF (32%). Winter season (JF) projections exhibit the highest variability across scenarios, ranging from an 11% decrease under SSP5-8.5 MF to a 14% increase under SSP5-8.5 FF, indicating complex climate dynamics that affect winter precipitation in the region. The pre-monsoon season (MAM) exhibits moderate but consistent increases across all scenarios, with the highest increase (18%) projected under SSP5-8.5 FF. These precipitation projections align with findings from Guhathakurta et al. (2020), who identified increasing trends in extreme precipitation events across southern peninsular India, particularly during the southwest monsoon season. The projected precipitation increases for Tirupati district are consistent with broader regional patterns identified in the Indian monsoon region under climate change scenarios (Krishnan et al., 2020).

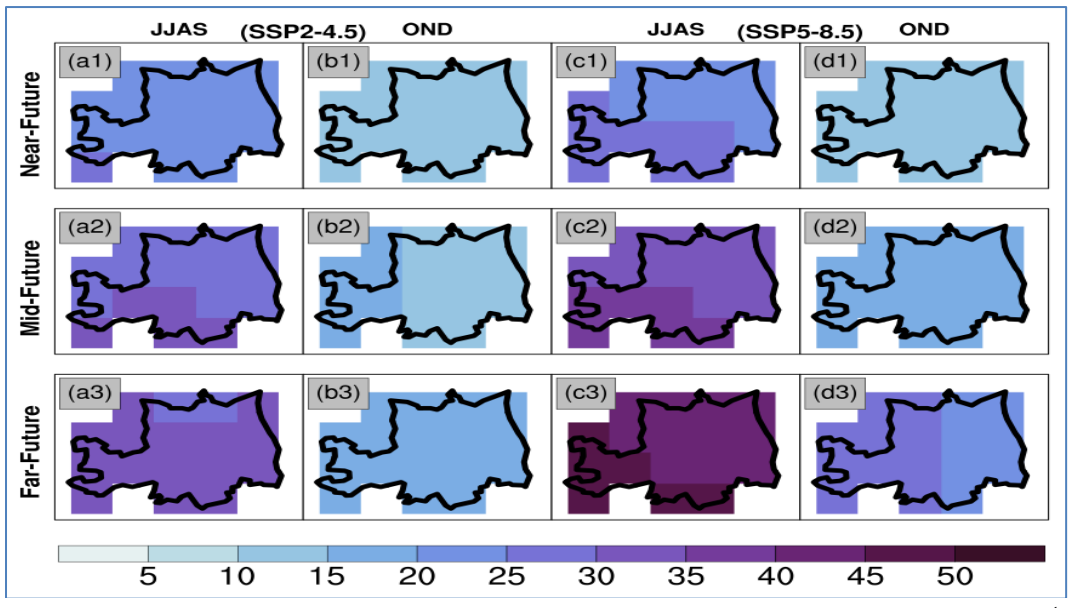
Figs. 8(b&c) demonstrate progressive warming across all time periods under both scenarios, with several key patterns emerging. T_{max} projections indicate annual increases ranging from 0.7 °C (SSP2-4.5 NF) to 3.2 °C (SSP5-8.5 FF). The T_{min} exhibits slightly higher warming rates than the maximum temperature under the SSP5-8.5 FF scenario, with annual increases reaching 3.4 °C. The most extreme warming is projected for the pre-monsoon season (MAM) under SSP5-8.5 FF, with both T_{max} and T_{min} increasing by 3.6 °C, suggesting particularly severe hot seasons. The southwest monsoon season (JJAS) shows marginally lower warming rates compared to other seasons, likely due to increased cloud cover and precipitation during this period. Both temperature parameters display a clear temporal progression of warming, with each successive time period showing higher temperature increases under the same emission scenario. The difference between SSP2-4.5 and SSP5-8.5 scenarios becomes increasingly pronounced in the mid and FF periods, highlighting the diverging climate consequences of different emission pathways. These temperature projections are consistent with those reported by Mishra et al. (2017), who projected significant increases in heat wave frequency and intensity across India under various warming scenarios. The pre-monsoon season warming is particularly concerning as it aligns with findings from Mukherjee et al. (2018), who documented amplified pre-monsoon warming trends across Southern India.

The combined projections for precipitation and temperature suggest complex climate change impacts for Tirupati district. The substantial increases in monsoon season precipitation, coupled with potential decreases in winter precipitation under some scenarios, indicate a likely intensification of seasonal water availability patterns. This will necessitate enhanced water storage infrastructure and management strategies, as highlighted

by Kumar et al. (2021). The pre-monsoon season, critical for many agricultural operations, faces the most severe warming projections. This warming, combined with variable precipitation changes, may significantly impact agricultural productivity& necessitate adjustments to cropping patterns, as suggested by Venkataraman et al. (2020). The projected increases in both maximum & minimum temperatures, particularly under SSP5-8.5, are likely to elevate heat-related health risks, especially during the pre-monsoon season when both temperature parameters exhibit the highest increases. This aligns with projections by Singh et al. (2023) regarding the differential impacts of heat exposure across southern Indian urban centres. The substantial differences between SSP2-4.5& SSP5-8.5 projections, particularly in the FF, emphasise the importance of mitigation efforts in determining the magnitude of climate change impacts in the region.

Similarly, the spatially explicit projections (supplementary Figs. S3-S12) provide crucial insights into the heterogeneity of climate change impacts within the district, which is essential for targeted adaptation planning at the sub-district level. Under both SSP2-4.5 and SSP5-8.5 scenarios, significant spatial and temporal variations in precipitation and temperature are projected for the district. the moderate SSP2-4.5 scenario, precipitation is projected to increase uniformly by 5-15% in the near NF, with the southwest monsoon (JJAS) contributing the most (10-20%), especially in northeastern parts. As the century progresses, spatial heterogeneity intensifies, with the MF increasing the shift toward the western district (15-25%) and further rising to 20-30% by 2076-2100. The southwest consistently receives the highest increases (supplementary Fig. S3). Winter (JF) shows more variable and less consistent changes. These spatially evolving patterns align with those reported by Vinnarasi et al. (2017), who found an increase in precipitation heterogeneity across South Indian districts under warming scenarios.

In contrast, SSP5-8.5 exhibits more intense and spatially differentiated precipitation changes. Near-future annual increases range between 10% and 20%, with JJAS again showing the largest rise. However, mid-future projections reveal a strong west-east gradient, with the western regions receiving 25-35% more rainfall, primarily during the JJAS period. This gradient intensifies in the future, with annual increases exceeding 40% in the west and extreme JJAS precipitation increases surpassing 50% (Supplementary Figure S5). Additional gains occur during the post-monsoon (OND) and winter (JF) seasons. These spatial patterns resemble those noted by Menon *et al.* (2020), who attributed such trends to altered monsoon dynamics under high emissions.



Figs. 9(a1-d3). Spatial heterogeneity of heavy rainfall days during monsoon seasons (JJAS and OND) for SSP2 (1st and 2nd columns) and SSP5 (3rd and 4th columns) for NF, MF and FF over Tirupati district

Temperature projections under both scenarios show consistent warming, with stronger signals under SSP5-8.5 (supplementary Fig. S8). Under SSP2-4.5, near-future annual T_{max} increases uniformly by 0.5-1.0 °C, rising to 1.0-1.5 °C in mid-future and 1.5-2.0 °C in FF (supplementary Fig. S6), with the pre-monsoon season (MAM) experiencing the highest seasonal warming (up to 2.2 °C). T_{min} follows a similar but more spatially uniform pattern, reaching 1.5-2.0 °C in the FF (supplementary Fig. S7), especially in northern areas during MAM and OND. These trends corroborate findings from Kothawale et al. (2016) and Vinnarasi and Dhanya (2018), who documented inland warming and relatively homogeneous T_{min} increases. SSP5-8.5 intensifies both T_{max} and T_{min} changes. T_{max} increases reach 1.5-2.5 °C in mid-future and up to 4.0 °C in far-future, particularly in the eastern district during MAM. T_{min} warming becomes more spatially differentiated, with a west-east gradient emerging in mid-future and strong nighttime warming (>3.5 °C) in the western regions during OND and JF in far-future. These patterns suggest rising risks for heat stress and agricultural productivity, consistent with projections by Mishra et al. (2017) and Sanjay et al. (2020), who highlighted the vulnerability of inland and nighttime temperatures to extreme warming in southern India.

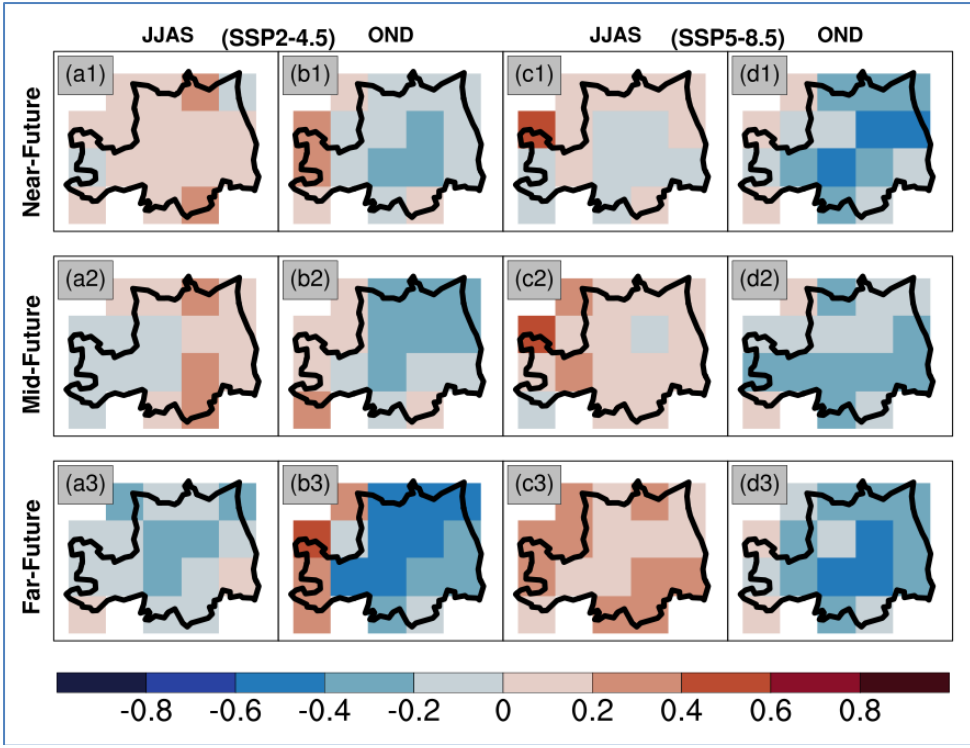
3.4. Spatial heterogeneity of climate indices over Tirupati district

Fig. 9 demonstrates projected changes in heavy rainfall days during the JJAS and OND seasons. Under both emission scenarios, there's a consistent increase in heavy rainfall days, particularly in the far-future period.

The SSP5-8.5 scenario exhibits more pronounced increases, with some areas anticipating up to 40-50 additional heavy rainfall days in the far future (Fig. 9c3). This aligns with the findings of Douville *et al.* (2021), which suggest an intensification of precipitation extremes under enhanced greenhouse warming. The spatial pattern indicates that the western parts of the district experience the most dramatic increases, particularly during the southwest monsoon (JJAS), with increases ranging from 15 to 25 days in the near future to 40 to 50 days in the far future under SSP5-8.5.

Fig. 10 illustrates changes in consecutive wet days, revealing a more complex and spatially heterogeneous pattern compared to the pattern of heavy rainfall days. Unlike the consistent increases observed for heavy precipitation events, consecutive wet days show mixed signals across the district. During the JJAS season, the eastern portions of Tirupati district generally show slight increases in consecutive wet days (1-3 additional days), while the western regions exhibit decreases of similar magnitude under both scenarios. This east-west gradient becomes more pronounced in the far future, particularly under SSP5-8.5. During the OND season, the pattern is more uniform, with most areas exhibiting modest increases in consecutive wet days (1-2 days) in the near future. However, this signal weakens and becomes more variable in later periods.

The contrasting patterns between Figs. 9 and 10 reveal an important characteristic of future precipitation changes over Tirupati: while the frequency of intense rainfall events increases substantially, the persistence of



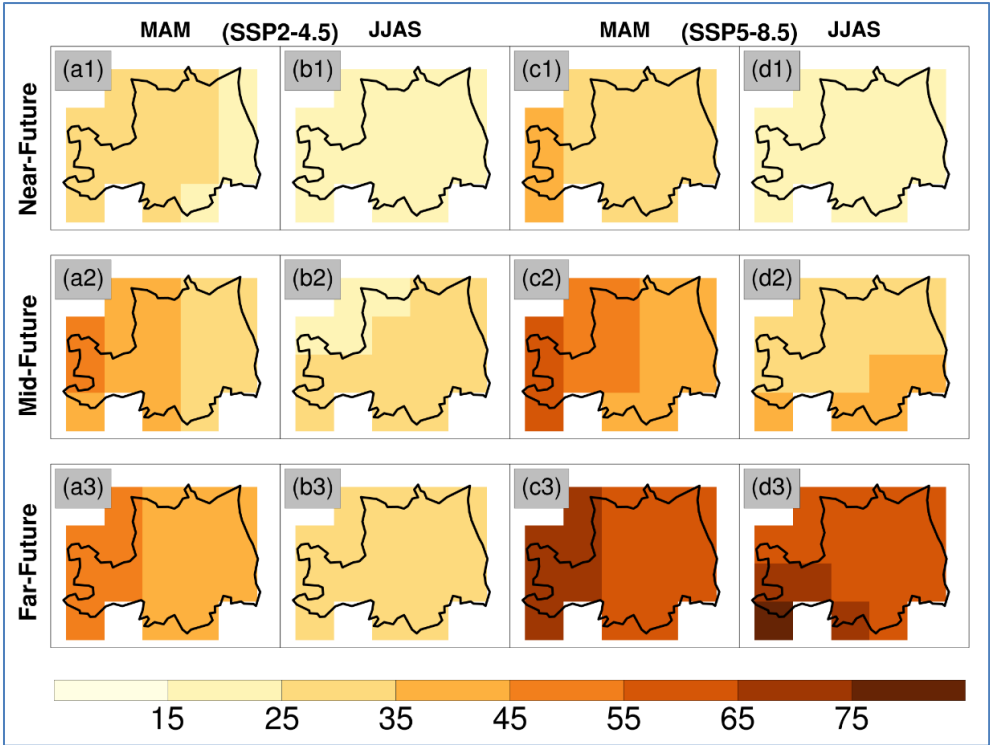
Figs. 10(a1-d3). Spatial heterogeneity of consecutive wet days during monsoon seasons (JJAS and OND) for SSP2 (1st and 2nd columns) and SSP5 (3rd and 4th columns) for NF, MF and FF over Tirupati district

wet conditions (consecutive wet days) does not follow the same trend. This suggests a shift toward more intermittent but intense precipitation patterns, where heavy rainfall occurs in shorter, more concentrated periods rather than extended wet spells. This finding corroborates research by Zhao *et al.* (2022), which indicates that changes in precipitation persistence can vary significantly at regional scales, even as average precipitation intensity increases.

Fig. 11 illustrates substantial increases in warm days during the MAM and JJAS seasons. The warming trend intensifies from near-future to far-future periods, with the SSP5-8.5 scenario exhibiting the most dramatic increases, ranging from 65 to 75 additional warm days in the far future [Figs.11(c3 & d3)]. The spatial distribution shows relatively uniform warming across the district during JJAS, but MAM exhibits a pronounced north-south gradient with northern areas experiencing 10-15 additional warm days than southern regions under the high-emission scenario. This warming pattern is consistent with findings from Fischer and Knutti (2015), which demonstrate that higher emission scenarios lead to more frequent heat extremes.

The concurrent analysis of these three climate indices reveals important relationships between precipitation patterns and warming:

- (i) Decoupling of precipitation intensity and persistence: While heavy rainfall days increase consistently across scenarios and periods (Fig. 9), consecutive wet days show complex, spatially variable changes (Fig. 10). This supports research by Trenberth et al. (2022), which indicates that warming increases water-holding atmospheric capacity, potentially intensifying precipitation when it occurs, but not necessarily increasing precipitation persistence.
- (2) Regional precipitation regime shifts: The inverse relationship between heavy rainfall days and consecutive wet days changes in western regions suggests a fundamental shift toward more intense but less persistent rainfall events. This pattern is consistent with findings from Cai et al. (2020) regarding changing precipitation characteristics under climate change, where the hydrological cycle becomes more episodic with longer dry periods punctuated by intense rainfall events.
- (3) Temperature-precipitation interactions: The uniform increase in warm days (Fig. 11) contrasts with the spatially heterogeneous precipitation patterns (Figs. 9 and 10), suggesting that local temperature responses to greenhouse warming are more predictable than precipitation responses, which are influenced by complex regional atmospheric dynamics.



Figs. 11(a1-d3). Spatial heterogeneity of warm days during summer and monsoon season (MAM and JJAS) for SSP2 (1st and 2nd columns) and SSP5 (3rd and 4th columns) for NF, MF and FF over Tirupati district.

(4) Scenario-dependent amplification: The most pronounced changes occur under the SSP5-8.5 scenario in the far-future period across all three indices, but the amplification factor varies by index. Heavy rainfall days exhibit the strongest scenario sensitivity, with SSP5-8.5 producing nearly twice the increase in many areas compared to SSP2-4.5, while consecutive wet days show less clear scenario differentiation.

These findings highlight the importance of mitigation efforts, as emphasised by Riahi *et al.* (2017) in their assessment of emissions scenarios, and underscore the need for adaptation strategies that account for both increased intensity and changed temporal distribution of precipitation events.

Moreover, the results show a consistent increase in both heavy rainfall days and warm days across other seasons in the projected timeframes (Supplementary Figs. S9-S12), with more pronounced changes in the FF period. These changes are more dramatic under the higher emission scenario than the moderate scenario. For heavy rainfall, the annual increases are most significant, reaching 20-30+ additional days in some regions, while seasonal changes (MAM, spring; JF, winter) show more modest

gains. For warm days, there's a striking progression across the time periods, with the western portion of the region experiencing the most severe increases, potentially exceeding 120 additional warm days annually in the FF under SSP5-8.5 (supplementary Fig. S12). The seasonal patterns for warm days show greater increases during spring (MAM) compared to winter (JF), suggesting pronounced seasonal shifts in temperature patterns over time.

4. Conclusions

Climate change impacts India's diverse geography and climate zones, causing unique challenges in each region. Addressing these challenges requires scientific research, effective policies, and community-based adaptation. Integrating climate resilience into national and regional planning safeguards vulnerable populations and ecosystems. Robust, region-specific climate adaptation strategies are urgently needed to account for changes in average conditions and extreme weather events, especially under higher emissions scenarios.

Projected changes in wet spell duration over major Indian cities are highly variable and region-specific, lacking the consistent upward trend seen in mean and heavy precipitation projections. This underscores the importance of analysing multiple precipitation indices to capture the complex nature of future hydrological changes and their potential impacts. These findings suggest that regions of historically low precipitation variability, particularly the Western Ghats and Himalayan foothills, are likely to experience the most significant absolute increases in rainfall, potentially straining coastal and upland hydrological systems. Meanwhile, areas already prone to large temperature swings, such as northwest India and the Himalayan belt, face compounded thermal risk that may exacerbate glacier and snow-melt sensitivities. Adaptation strategies must therefore account for decoupling historical variability hotspots from future wetting maxima, tailoring water-resource, agricultural, and infrastructure planning to the distinct climate trajectories of each subregion.

The projected increases in warm days and heavy rainfall suggest an intensification of the hydrological cycle over Tirupati district, potentially leading to an increased risk of floods and droughts. This aligns with IPCC AR6 findings (Seneviratne et al., 2021) on compound climate extremes. These results have a significant impact on the region's water resource management, agriculture, and disaster preparedness, necessitating adaptive strategies that account for increased warming and changing precipitation patterns. These spatially differentiated climate change impacts underscore the need for localised adaptation strategies within the Tirupati district, as suggested by Krishnan et al. (2020) in their assessment of regional climate change impacts across India. Under moderate (SSP2-4.5) and high-emission (SSP5-8.5) scenarios, precipitation increases across the district, with the western regions experiencing the most substantial increases, particularly during the monsoon season. The high-emission scenario shows more pronounced spatial patterns and higher magnitudes of precipitation change. Temperature increases are also projected, with the eastern portions of the district experiencing the most extreme warming, especially during the pre-monsoon season.

The spatial analysis reveals several key vulnerability hotspots within the Tirupati district.

- (i) Western sub-districts: These areas face the most dramatic increases in monsoon precipitation (>50% under SSP5-8.5 in the FF), suggesting increased flood risks and potential for soil erosion. However, they show slightly lower temperature increases compared to eastern regions.
- (ii) Eastern sub-districts: These areas experience the most extreme maximum temperature increases, particularly during the pre-monsoon season. This could

have a significant impact on agricultural productivity and human health. Combining high temperatures with moderate precipitation suggests potential heat stress and water management challenges.

(iii) Northern sub-districts: These areas show the highest minimum temperature increases under several scenarios, which could impact agricultural productivity through impacts on nighttime plant respiration and development processes.

From a policy perspective, shifting from SSP5 to SSP2 can avert tens of extra warm days annually and reduce end-of-century T_{max} and T_{min} by approximately 1-1.5 °C. This mitigation dividend is most significant in the future, but meaningful reductions also accrue by midcentury, limiting cumulative health impacts during the most rapidly warming decades. Integrating these projections into urban planning, public health preparedness, and emissions reduction commitments will be crucial to safeguard India's rapidly growing cities against intensifying heat hazards. The differential impacts across these three crucial South Indian cities highlight the need for location-specific climate adaptation strategies. The emissions pathways represented by the SSP scenarios will significantly influence the severity of climate impacts, with the higher-emission SSP5-8.5 scenario leading to more extreme changes than the moderate SSP2-4.5 scenario.

As Venkataraman et al. (2018) have demonstrated, emission pathways will substantially determine future air quality and climate conditions across India, with important implications for policy decisions. The projected climate changes for Tirupati district reveal a future characterised by increased precipitation, particularly during the monsoon season, alongside substantial warming across all seasons. These changes will likely present significant challenges for the region's water resource management, agriculture, human health, and infrastructure. The marked differences between moderate (SSP2-4.5) and high-emission (SSP5-8.5) scenarios underscore the importance of global mitigation efforts in determining the severity of these regional climate impacts. The spatial patterns presented in these projections were derived from downscaled global climate models, which inherently contain uncertainties, particularly at fine spatial scales. The transparent spatial gradients in the far-future projections under the high-emission scenario should be interpreted cautiously, as Ramesh and Goswami (2022) noted in their evaluation of downscaled climate projections for South Indian regions.

The findings emphasise the urgency of implementing adaptation measures, enhancing climate resilience, and

integrating climate risk management into development planning. These findings underscore the need for tailored adaptation planning and infrastructure resilience measures for specific regional projections in urban centres. Increased mean annual rainfall and a disproportionately larger increase in heavy rainfall days signal heightened risks of hydro-climatic hazards, such as urban flooding, landslides, and infrastructure damage, in major Indian cities. Extreme events pose significant challenges to urban planning, drainage systems, and disaster management.

Data availability

All data used in the study are freely available from the sources mentioned in the data section. Rainfall data can be obtained from the India Meteorological Department (https://www.imdpune.gov.in/cmpg/Griddata/Rainfall_25_NetCDF.html), and temperature (https://www.imdpune.gov.in/cmpg/Griddata/Max_1_Bin. html). NEX-GDDP data is downloaded from https://ds.nccs.nasa.gov/thredds/catalog/AMES/NEX/GD DP-CMIP6/catalog.html.

Code availability

The analysis utilisedPyferret, developed by the Pacific Marine Environmental Laboratory, National Oceanic and Atmospheric Administration (https://ferret.pmel.noaa.gov/Ferret), as well as Python, CDO, MATLAB, R Studio, and NCL. The codes used in this study are available upon request from the corresponding author.

Acknowledgements

VT thanks Prof. Anna Rutgersson, Department of Earth Sciences, Uppsala University and GreenFeedBack, an EU-HORIZON project (101056921), for the support the research infrastructure provided. acknowledges the resources provided by Uppsala University, the National Academic Infrastructure for Supercomputing in Sweden (NAISS), and the Swedish National Infrastructure for Computing (SNIC) at Uppsala and Chalmers Universities, partially funded by the Swedish Research Council through grant agreement no. 2022-06725 and no. 2018-05973. The authors thank IMD and NEX-GDDP-CMIP6 for providing data and software support, including CDO, Pyferret, NCL, R Studio, Python, and Microsoft. Authors are also thankful to Google Maps.

Authors' Contributions

Venkatramana Kaagita: formulated the research idea and contributed equally to data processing, analysis, figure generation, and preparation of the first draft.

Venugopal Thandlam: formulated the research idea and contributed equally to data processing, analysis, figure generation, and preparation of the first draft.

Venkatramana Reddy Sakirevupalli: Refined the draft and shaped the present work into its final form.

Byju Pookkandy: Refined the draft and shaped the present work into its final form.

Gari Sarojamma: Refined the draft and shaped the present work into its final form.

Disclaimer: The contents and views presented in this research article/paper are the views of the authors and do not necessarily reflect the views of the organizations they belong to.

References

- Ali, H., Mishra, V., and Pai, D. S., 2021, "Observed and projected urban extreme rainfall events in India", *J. Geophys. Res. Atmos.*, **126**, 5, e2020JD033554. https://doi.org/10.1029/2020JD033554.
- Allen, S. K., Rastner, P., Arora, M., Huggel, C. and Stoffel, M., 2016, "Lake outburst and debris flow disaster at Kedarnath, June 2013: Hydrometeorological triggering and topographic predisposition", *Nat. Hazards Earth Syst. Sci.*, **16**, 6, 1325–1340. https://doi.org/10.5194/nhess-16-1325-2016.
- Almazroui, M., Saeed, F., Saeed, S., Ismail, M., Ehsan, M.A., Diallo, I., O'Brien, E., Ashfaq, M., Martínez-Castro, D. and Cavazos, T., 2020, "Projected changes in temperature and precipitation over the United States, Central America, and the Caribbean in CMIP6 GCMs", Atmosphere ,11, 10, 1096. https://doi.org/ 10.3390/atmos11101096.
- Anstey, J. A. and Shepherd, T. G., 2014, "High-latitude influence of the quasi-biennial oscillation", *Q. J. R. Meteorol. Soc.*, **140**, 679, 1–21. https://doi.org/10.1002/qj.2132.
- Ashok, K., Guan, Z., Saji, N. H., and Yamagata, T 2004, "Individual and combined influences of ENSO and the Indian Ocean Dipole on the Indian summer monsoon", *J. Clim.*, **20**, 14, 3147–3160. https://doi.org/10.1175/JCLI4161.1.
- Baldwin, M. P., Gray, L. J., Dunkerton, T. J., Hamilton, K., Haynes, P.H., Randel, W.J., Holton, J.R., Alexander, M.J., Hirota, I., Horinouchi, T. and Jones, D.B.A., 2001, "The quasi-biennial oscillation", Rev. Geophys., 39, 2, 179–229. https://doi.org/ 10.1029/1999RG000073.
- Bolch, T., Kulkarni, A., Kääb, A., Bolch, T., Kulkarni, A., Kääb, A., Huggel, C., Paul, F., Cogley, J.G., Frey, H., Kargel, J.S., Fujita, K., Scheel, M. and Bajracharya, S., 2012, "The state and fate of Himalayan glaciers", *Science*, **336**, 6079, 310–314. https://doi.org/10.1126/science.1215828.
- Cai, W., McPhaden, M. J., Grimm, A. M., Rodrigues, R.R., Taschetto, A.S., Garreaud, R.D., Dewitte, B., Poveda, G., Ham, Y.G., Santoso, A. and Ng, B., 2020, "Climate impacts of the El Niño— Southern Oscillation on South America", *Nat. Rev. Earth Environ.*, 1, 4, 215–231. https://doi.org/10.1038/s43017-020-0040-3.
- Chaubey, P. K., Mall, R., Jaiswal, R., and Payra, S., 2022, "Spatio-temporal changes in extreme rainfall events over different Indian River Basins". *Earth and Space Science*, **9**, 3, e2021EA001930. https://doi.org/10.1029/2021ea001930
- Dai, A. and Zhao, T., 2017, "Uncertainties in historical changes and future projections of drought. Part I: Estimates of historical

- drought changes", *Clim. Change*, **144**, 3, 519–533. https://doi.org/10.1007/s10584-016-1705-2.
- Dash, S. K., Kulkarni, M. A., Mohanty, U. C., and Prasad, K., 2009, "Changes in the characteristics of rain events in India", J. Geophys. Res. Atmos., 114, D10. https://doi.org/ 10.1029/2008JD010572.
- Dhanya, P. and Ramachandra, T. V., 2016, "Carbon sequestration potential of the forest ecosystems in the Western Ghats, a global biodiversity hotspot", *Nat. Resour. Res.*, 25, 4, 443-456. https://doi.org/10.1007/s11053-016-9288-1.
- Douville, H., Raghavan, K., Renwick, J., 2023, "Climate Change 2021: The Physical Science Basis. Contribution of Working Group I to the Sixth Assessment Report of the Intergovernmental Panel on Climate Change", Cambridge University Press, 1055–1210. https://doi.org/10.1017/9781009157896.010.
- Dubey, A. K., Lal, P., Kumar, P., and Dvornikov, A.Y., 2021, "Present and future projections of heatwave hazard-risk over India: A regional earth system model assessment", *Environ. Res.*, 201, 111573. https://doi.org/10.1016/j.envres.2021.111573.
- Dubey, S. K., Sharma, A., and Singh, R., 2021, "Future projections of Indian summer monsoon rainfall using a high-resolution regional climate model", Clim. Dyn., 56, 11-12, 3457–3472. https://doi.org/10.1007/s00382-021-05602-3.
- Enfield, D. B., Mestas-Nuñez, A. M., and Trimble, P. J., 2001, "The Atlantic multidecadal oscillation and its relation to rainfall and river flows in the continental U.S.", *Geophys. Res. Lett.*, 28, 10, 2077–2080. https://doi.org/10.1029/2000GL012745.
- Eyring, V., Bony, S., Meehl, G. A., Senior, C.A., Stevens, B., Stouffer, R.J. and Taylor, K.E., 2016, "Overview of the Coupled Model Intercomparison Project Phase 6 (CMIP6) experimental design and organisation", *Geosci. Model Dev.*, 9, 5, 1937–1958. https://doi.org/10.5194/gmd-9-1937-2016.
- Fischer, E. M. and Knutti, R., 2015, "Anthropogenic contribution to global occurrence of heavy-precipitation and high-temperature extremes", *Nat. Clim. Change*, 5, 6, 560–564. https://doi.org/ 10.1038/nclimate2617.
- Gadgil, S., 2003, "The Indian monsoon and its variability", Annu. Rev. Earth Planet. Sci., 31, 429–467. https://doi.org/10.1146/annurev. earth.31.100901.141251.
- Guhathakurta, P., Khedikar, S., Menon, P., Prasad, A.K., Sangwan, N. and Advani, S.C., 2020, "Observed rainfall variability and changes over Andhra Pradesh state", *Meteorol. Monogr.*, ESSO/IMD/HS/Rainfall Variability/22(2020)/44. https://doi.org/10.54302/mausam.y73i1.5340.
- Gusain, A., Ghosh, S., and Karmakar, S., 2020, "Added value of CMIP6 over CMIP5 models in simulating Indian summer monsoon rainfall", Clim. Dyn.,54, 3-4, 1849–1866. https://doi.org/ 10.1007/s00382-020-05359-3.
- Hallegatte, S., 2016, "Shock waves: Managing the impacts of climate change on poverty", World Bank Publications. https://doi.org/ 10.1596/978-1-4648-0673-5.
- Hazra, S., Ghosh, T., DasGupta, R., and Sen,G., 2002, "Sea level and associated changes in the Sundarbans", Sci. Cult., 68, 9-12, 309-321.
- Hrudya, P. H., Varikoden, H., and Vishnu, R., 2021, "A review on the Indian summer monsoon rainfall, variability and its association with ENSO and IOD", *Meteorol. Atmos. Phys.*, **133**, 1–14. https://doi.org/10.1007/s00703-020-00720-0.
- Indian Meteorological Department, 2022, "Annual Report 2022", IMD. https://www.imd.gov.in/annual-report-2022.
- IPCC, 2021, "Climate Change 2021: The Physical Science Basis. Contribution of Working Group I to the Sixth Assessment

- Report of the Intergovernmental Panel on Climate Change", *Cambridge University Press.* https://doi.org/10.1017/9781009157896.
- Kim, H., Ye, A., and Kim, T. W., 2020, "Evaluation of CMIP6 multi-model ensemble for extreme precipitation indices over East Asia", Clim. Dyn., 55, 3–4, 1015–1029. https://doi.org/10.1007/s00382-020-05400-3.
- Knight, J. R., Folland, C. K., and Scaife, A. A., 2006, "Climate impacts of the Atlantic Multidecadal Oscillation", Geophys. Res. Lett., 33, 17, L17706. https://doi.org/10.1029/2006GL026242.
- Kothawale, D. R., Deshpande, N. R., and Kolli, R. K., 2016, "Long term temperature trends at major, medium, small cities and hill stations in India during the period 1901–2013", *Am. J. Clim. Change*, **5**, 3, 383–398. https://doi.org/10.4236/ajcc.2016.53029.
- Krishnan, R., Sanjay, J., Gnanaseelan, C., Mujumdar, M., Kulkarni, A. and Chakraborty, S., 2020, "Assessment of climate change over the Indian region", *Springer*. https://doi.org/10.1007/978-981-15-4327-2.
- Krishnan, R., Shrestha, A. B., Ren, G., Rajbhandari, R., Saeed, S., Sanjay, J., Syed, M.A., Vellore, R., Xu, Y., You, Q. and Ren, Y., 2019, "Unravelling climate change in the Hindu Kush Himalaya: Rapid warming in the mountains and increasing extremes", In The Hindu Kush Himalaya Assessment: Mountains, Climate Change, Sustainability and People, Springer, 57–97. https://doi.org/10.1007/978-3-319-92288-1_3.
- Kumar, P., Debele, S. E., Sahani, J., Rawat, N., Marti-Cardona, B., Alfieri, S.M., Basu, B., Basu, A.S., Bowyer, P., Charizopoulos, N. and Gallotti, G., 2021, "Nature-based solutions efficiency evaluation against natural hazards: Modelling methods, advantages and limitations", Sci. Total Environ., 784, 147058. https://doi.org/10.1016/j.scitotenv.2021.147058.
- Lobell, D. B., Schlenker, W., and Field, C. B., 2012, "Climate trends and global crop production since 1980", *Science*, 333, 6051, 616–620. https://doi.org/10.1126/science.1204030.
- Mahapatra, M., Ramakrishnan, R., and Rajawat, A. S., 2015, "Coastal vulnerability assessment of Gujarat coast to sea level rise using GIS techniques: A preliminary study", *J. Coast. Conserv.*, **19**, 241–256. https://doi.org/10.1007/s11852-015-0384-x.
- Mantua, N. J., Hare, S. R., Zhang, Y., Wallace, J.M. and Francis, R.C., 1997, "A Pacific interdecadal climate oscillation with impacts on salmon production", *Bull. Am. Meteorol. Soc.*, 78, 6, 1069–1079. https://doi.org/10.1175/1520-0477(1997)078<1069: APICOW>2.0.CO;2.
- Mathison, C., Wiltshire, A., Falloon, P., and Challinor, A.J., 2015, "South Asia river-flow projections and their implications for water resources", *Hydrol. Earth Syst. Sci.*, 19, 12, 4783-4810 . https://doi.org/10.5194/hess-19-2325-2015.
- McPhaden, M. J., Zebiak, S. E., and Glantz, M. H., 2006, "ENSO as an integrating concept in Earth science", *Science*, **314**, 5806, 1740–1745. https://doi.org/10.1126/science.1132588.
- Menon, A., Levermann, A., and Schewe, J., 2020, "Enhanced future variability during India's rainy season", *Philos. Trans. R. Soc.* A, 378, 2191, 20190521. https://doi.org/10.1098/rsta.2019.0521.
- Mirza, M. M. Q., 2002, "Global warming and changes in the probability of occurrenceof floods in Bangladesh and implications", *Glob. Environ. Change*, 12, 2, 127–138. https://doi.org/10.1016/ S0959-3780(02)00002-X.
- Mishra, V. and Shah, H. L., 2018, "Hydroclimatological perspective of the Kerala flood of 2018", J. Geol. Soc. India, 92, 645–650. https://doi.org/10.1007/s12594-018-1079-3.
- Mishra, V., Mukherjee, S., Kumar, R., and Stone, D.A., 2017, "Heat wave exposure in India in current, 1.5 °C, and 2.0 °C worlds",

- Environ. Res. Lett., 15, 10, 104009. https://doi.org/10.1088/1748-9326/aba4d5.
- Mishra, V., Shah, R., Azhar, S., Shah, H., Modi, P. and Kumar, R., 2018, "Reconstruction of droughts in India using multiple land-surface models (1951–2015)", *Hydrol. Earth Syst. Sci.*, 22, 4, 2269– 2284. https://doi.org/10.5194/hess-22-2269-2018.
- Mishra, V., Vellore, R., and Kumar, D. N., 2020, "Future heatwaves over India: Hazard scenarios and climate change implications", *Environ. Res.*, 182, 109110. https://doi.org/10.1016/ j.envres.2019.109110.
- Mohanty, A., Dubey, A., and Singh, R. B., 2022, "Cyclonic disasters and resilience", *Springer*, Singapore.
- Mohanty, P. K., Kar, P. K., and Behera, B., 2020, "Impact of very severe cyclonic storm Phailin on shoreline change along South Odisha Coast", Nat. Hazards, 102, 633–644.
- Mujumdar, M., Bhaskar, P., Ramarao, M.V.S., Uppara, U., Goswami, M., Borgaonkar, H., Chakraborty, S., Ram, S., Mishra, V., Rajeevan, M. and Niyogi, D., 2020, "Droughts and floods. In Assessment of climate change over the Indian region", a report of the Ministry of Earth Sciences (MoES), Government of India (pp. 117-141).
- Mukherjee, S., Mishra, A., and Trenberth, K. E., 2018, "Climate change and drought: A perspective on drought indices", Curr. Clim. Change Rep., 4, 2, 145–163. https://doi.org/10.1007/s40641-018-0098-x.
- Newman, M., Alexander, M. A., Ault, T. R., Cobb, K.M., Deser, C., Di Lorenzo, E., Mantua, N.J., Miller, A.J., Minobe, S., Nakamura, H. and Schneider, N., 2016, "The Pacific Decadal Oscillation, revisited", J. Clim., 29, 12, 4399–4427. https://doi.org/10.1175/ JCLI-D-15-0508.1.
- Nishimoto, E. and Yoden, S., 2017, "Influence of the stratospheric quasibiennial oscillation on the Madden-Julian Oscillation", *Geophys. Res. Lett.*, **44**, 15, 7789–7795. https://doi.org/10.1002/ 2017GL074806.
- O'Brien, K., Leichenko, R., Kelkar, U., Venema, H., Aandahl, G., Tompkins, H., Javed, A., Bhadwal, S., Barg, S., Nygaard, L. and West, J., 2004, "Mapping vulnerability to multiple stressors: Climate change and globalization in India", *Glob. Environ. Change*, 14, 4, 303–313. https://doi.org/10.1016/j.gloenvcha.2004.07.001.
- Pfahl, S., O'Gorman, P. A., and Fischer, E. M., 2017, "Understanding the regional pattern of projected future changes in extreme precipitation", *Nat. Clim. Change*, 7, 5, 423–427. https://doi.org/ 10.1038/nclimate3287.
- Prakash, S., Mitra, A. K., Momin, I. M., Rajagopal, E.N., Basu, S., Collins, M., Turner, A.G., Achuto Rao, K. and Ashok, K., 2015, "Seasonal intercomparison of observational rainfall datasets over India during the southwest monsoon season", *Int. J. Climatol.*, 35, 9, 2326–2338. https://doi.org/10.1002/joc.4129.
- Raghavan, M., Barocas, S., Kleinberg, J., and Levy, K., 2020, 2020, "Mitigating bias in algorithmic hiring: Evaluating claims and practices", *In ACM Conference on Fairness*, Accountability, and Transparency (FAT). https://doi.org/10.2139/ssrn.3408010.
- Ramachandran, A., Praveen, D., Jaganathan, R., Raviraj,A., 2017, "Observed climate variability and change in Tiruchirappalli district, Tamil Nadu, India", *Meteorol. Appl.*, **24**, 3, 494–504. https://doi.org/10.1002/met.1651.
- Ramesh, B. R., Swaminathan, R., and Ganeshaiah, K. N., 2015, "Forest fire risk and its impact on biodiversity in the Western Ghats", For. Ecol. Manag., 341, 29–38. https://doi.org/10.1016/ j.foreco.2014.12.029.
- Ramesh, K. V. and Goswami, P., 2022, "Assessing reliability of regional climate projections: The case of Indian monsoon", Sci. Rep., 12, 2091. https://doi.org/10.1038/s41598-022-05814-7.

- Rangwala, I. and Miller, J. R., 2012, "Climate change in mountains: A review of elevation-dependent warming and its possible causes", Clim. Change, 114, 527–547. https://doi.org/10.1007/ s10584-012-0419-3.
- Rao, A. D., Upadhaya, P., Ali, H., Pandey, S. and Warrier, V., 2020, "Coastal inundation due to tropical cyclones along the east coast of India: An influence of climate change impact", *Nat. Hazards*, 101, 39–57.
- Rao, K. K., Reddy, P. J., and Chowdary, J. S., 2023, "Indian heatwaves in a future climate with varying hazard thresholds", *Environ. Res. Clim.*, 2, 1, 015002.
- Revi, A., Satterthwaite, D. E., Aragón-Durand, F., Corfee-Morlot, J., Kiunsi, R.B., Pelling, M., Roberts, D.C. and Solecki, W., 2014, "Urban areas", In Climate Change 2014: Impacts, Adaptation, and Vulnerability. Part A: Global and Sectoral Aspects", Cambridge University Press, 535–612. https://doi.org/10.1017/ CBO9781107415379.013.
- Riahi, K., van Vuuren, D. P., Kriegler, E., Edmonds, J., O'neill, B.C., Fujimori, S., Bauer, N., Calvin, K., Dellink, R., Fricko, O. and Lutz, W., 2017, "The Shared Socioeconomic Pathways and their energy, land use, and greenhouse gas emissions implications: An overview", Glob. Environ. Change, 42, 153–168. https://doi.org/10.1016/j.gloenvcha.2016.05.009.
- Rohini, P., Rajeevan, M., and Mukhopadhay, P., 2019, "Future projections of heat waves over India from CMIP5 models", *Clim. Dyn.*, **53**, 975–988. https://doi.org/10.1007/s00382-019-04661-z.
- Roxy, M. K., Ghosh, S., Pathak, A., Athulya, R., Mujumdar, M., Murtugudde, R., Terray, P. and Rajeevan, M., 2017, "A threefold rise in widespread extreme rain events over central India", Nat. Commun., 8, 708. https://doi.org/10.1038/s41467-017-00744-9.
- Saji, N., Goswami, B., Vinayachandran, P., and Yamagata, T., 1999, "A dipole mode in the tropical Indian Ocean", *Nature*, 401, 360– 363. https://doi.org/10.1038/43854.
- Sanjay, J.,Revadekar, J.V., Ramarao, M.V.S., Borgaonkar, H., Sengupta, S., Kothawale, D.R., Patel, J., Mahesh, R., Ingle, S., AchutaRao, K. and Srivastava, A.K., 2020, "Downscaling of CMIP5 Global Climate Models for Regional Climate Projections over India", In Assessment of Climate Change over the Indian Region, Springer, Singapore, 21–42. https://doi.org/10.1007/978-981-15-4327-2_2.
- Seneviratne, S. I., Zhang, X., Adnan, M., Badi, W., Dereczynski, C., Luca, A.D., Ghosh, S., Iskandar, I., Kossin, J., Lewis, S. and Otto, F., 2021, "Climate Change 2021: The Physical Science Basis. Contribution of Working Group I to the Sixth Assessment Report of the Intergovernmental Panel on Climate Change", Cambridge University Press, 1513–1766. https://doi.org/10.1017/9781009157896.013.
- Shrestha, A. B., Wake, C. P., Mayewski, P. A., and Dibb,J.E., 1999, "Maximum temperature trends in the Himalaya and its vicinity: An analysis based on temperature records from Nepal for the period 1971–94", *J. Clim.*,12, 2775–2786. https://doi.org/10.1175/1520-0442(1999)012<2775:MTTITH> 2.0.CO;2.
- Sillmann, J., Kharin, V. V., Zhang, X., Zwiers, F.W. and Bronaugh, D., 2013, "Climate extremes indices in the CMIP5 multimodel ensemble: Part 1. Model evaluation in the present climate", J. Geophys. Res. Atmos., 118, 4, 1716–1733. https://doi.org/ 10.1002/jgrd.50203.
- Singh, C., Urpelainen, J., and Srinivasan, J., 2023, "Comparing the exposure to heatwaves of slum versus non-slum areas in Bangalore, India", Environ. Res. Lett., 18, 6, 064039. https://doi.org/10.1088/1748-9326/acd2b3.

- Srinivasan, J. and Sibi, K., 2021, "Analysis and impact assessment of urban heat islands over Chennai Metropolitan Area using multisensor/source data and geospatial technologies", *Ecol. Indic.*, **133**, 108352. https://doi.org/10.1016/j.ecolind. 2021.108352.
- Tebaldi, C. and Knutti, R., 2007, "The use of the multi-model ensemble in probabilistic climate projections", *Philos. Trans. R. Soc. A*, **365**, 1857, 2053–2075. https://doi.org/10.1098/rsta.2007.2076.
- Thandlam, V., Kaagita, V., and Venkatramanareddy, S., 2024, "Long-term meteorological characteristics and extreme climate indices over Tirupati: A rapidly developing tropical city", *Discov. Cities*, 1, 1, 14. https://doi.org/10.1007/s44327-024-00013-7.
- Trenberth, K. E., 1997, "The definition of El Niño", *Bull. Am. Meteorol. Soc.*, **78**, 12, 2771–2777. https://doi.org/10.1175/1520-0477(1997)078<2771:TDOENO>2.0.CO;2.
- Trenberth, K. E., Cheng, L., Abraham, J. P., Trenberth, K.E., Mann, M.E., Zanna, L., England, M.H., Zika, J.D., Fasullo, J.T., Yu, Y. and Pan, Y., 2022, "Past and future ocean warming", *Nat. Rev. Earth Environ.*, 3, 11, 776–794. https://doi.org/10.1038/s43017-021-00261-x.
- Turner, A. G. and Annamalai, H., 2012, "Climate change and the South Asian summer monsoon", Nat. Clim. Change, 2, 8, 587–595. https://doi.org/10.1038/nclimate1495.
- Venkataraman, C., Brauer, M., Tibrewal, K., Sadavarte, P., Ma, Q., Cohen, A., Chaliyakunnel, S., Frostad, J., Klimont, Z., Martin, R.V. and Millet, D.B., 2018, "Source influence on emission pathways and ambient PM2.5 pollution over India (2015– 2050)", Atmos. Chem. Phys., 18, 12, 8017–8039.
- Venkataraman, M., Raju, B.M.K., Rao, A.V.M., Rao, K.V., Samuel, J., Ramachandran, K., Nagasree, K., Kumar, R.N. and Shankar, K.R. 2020, "District level agro-climatic vulnerability

- assessment of Andhra Pradesh to climate change", *J. Agrometeorol.*, **22**, 4, 387–395. https://doi.org/10.54386/jam.y22i4.178.
- Vinnarasi, R. and Dhanya, C. T., 2018, "Changing characteristics of extreme wet and dry spells of Indian monsoon rainfall", J. Geophys. Res. Atmos., 123, 5, 2737–2754. https://doi.org/10. 1002/2017JD027731.
- Vinnarasi, R., Dhanya, C. T., Chakravorty, A., 2017, "Unravelling rainfall extremes at the regional scale in the Indian Peninsular using a non-parametric regionalisation scheme", *Int. J. Climatol.*, 37, 911–923. https://doi.org/10.1002/joc.4758.
- Vitart, F., 2017, "Madden–Julian Oscillation prediction and teleconnections in the S2S database", Q. J. R. Meteorol. Soc., 143, 703, 2066–2079. https://doi.org/10.1002/qj.3079.
- Wang, B., Wu, R., and Fu, X., 2001, "Pacific–East Asian teleconnection: How does ENSO affect East Asian climate?", *J. Clim.*, **13**, 9, 1517–1536. https://doi.org/10.1175/1520-0442(2000)013<1517: PEATHD>2.0.CO;2.
- Webster, P., Moore, A., Loschnigg, J., and Leben, R.R., 1999, "Coupled ocean–atmosphere dynamics in the Indian Ocean during 1997–98", *Nature*, **401**, 356–360. https://doi.org/10.1038/43848.
- Yaduvanshi, A., Nkemelang, T., Bendapudi, R., and New, M., 2021, "Temperature and rainfall extremes change under current and future global warming levels across Indian climate zones", Weather Clim. Extrem., 31, 100291.
- Zhang, C., 2005, "Madden–Julian Oscillation", *Rev. Geophys.*, **43**, 2, RG2003. https://doi.org/10.1029/2004RG000158.
- Zhao, M., 2022, "A study of AR-, TS-, and MCS-associated precipitation and extreme precipitation in present and warmer climates", J. Clim., 35, 2, 479–497. https://doi.org/10.1175/JCLI-D-21-0145.1.

Appendix

TABLE S1

List of models used in the study

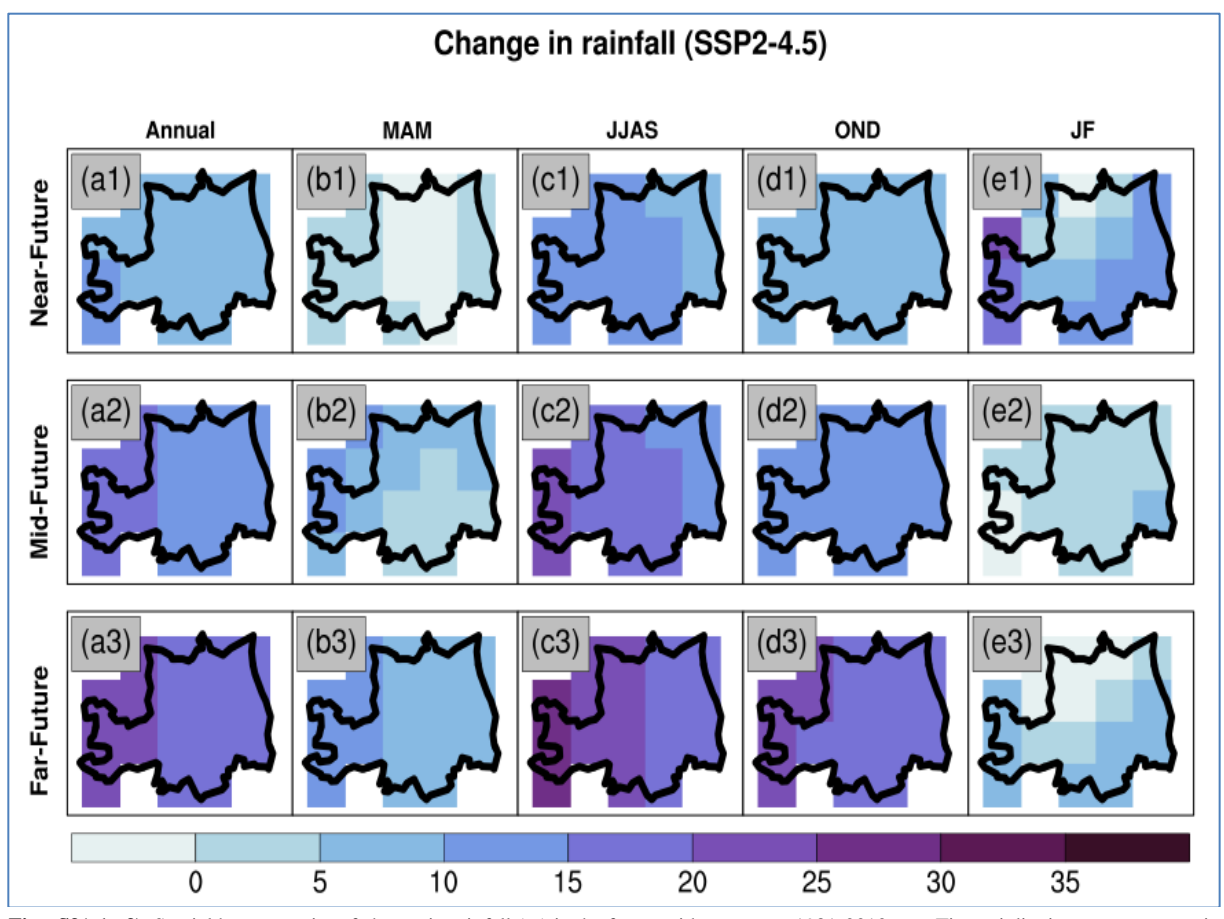
S.No	Model Name	Country	S.No	Model Name	Country
1	ACCESS-CM2	Australia	16	INM-CM4-8	Russia
2	ACCESS-ESM1-5	Australia	17	INM-CM5-0	Russia
3	BCC-CSM2-MR	China	18	IPSL-CM6A-LR	France
4	CanESM5	Canada	19	KACE-1-0-G	South Korea
5	CMCC-CM2-SR5	Italy	20	KIOST-ESM	South Korea
6	CMCC-ESM2	Italy	21	MIROC6	Japan
7	CNRM-CM6-1	France	22	MIROC-ES2L	Japan
8	CNRM-ESM2-1	France	23	MPI-ESM1-2-HR	Germany
9	EC-Earth3	Europe	24	MPI-ESM1-2-LR	Germany

S.No	Model Name	Country	S.No	Model Name	Country
10	EC-Earth3-Veg-LR	Europe	25	MRI-ESM2-0	Japan
11	FGOALS-g3	China	26	NESM3	China
12	GFDL-CM4_gr2	United States	27	NorESM2-LM	Norway
13	GFDL-CM4	United States	28	NorESM2-MM	Norway
14	GFDL-ESM4	United States	29	UKESM1-0-LL	United Kingdom
15	HadGEM3	United Kingdom			

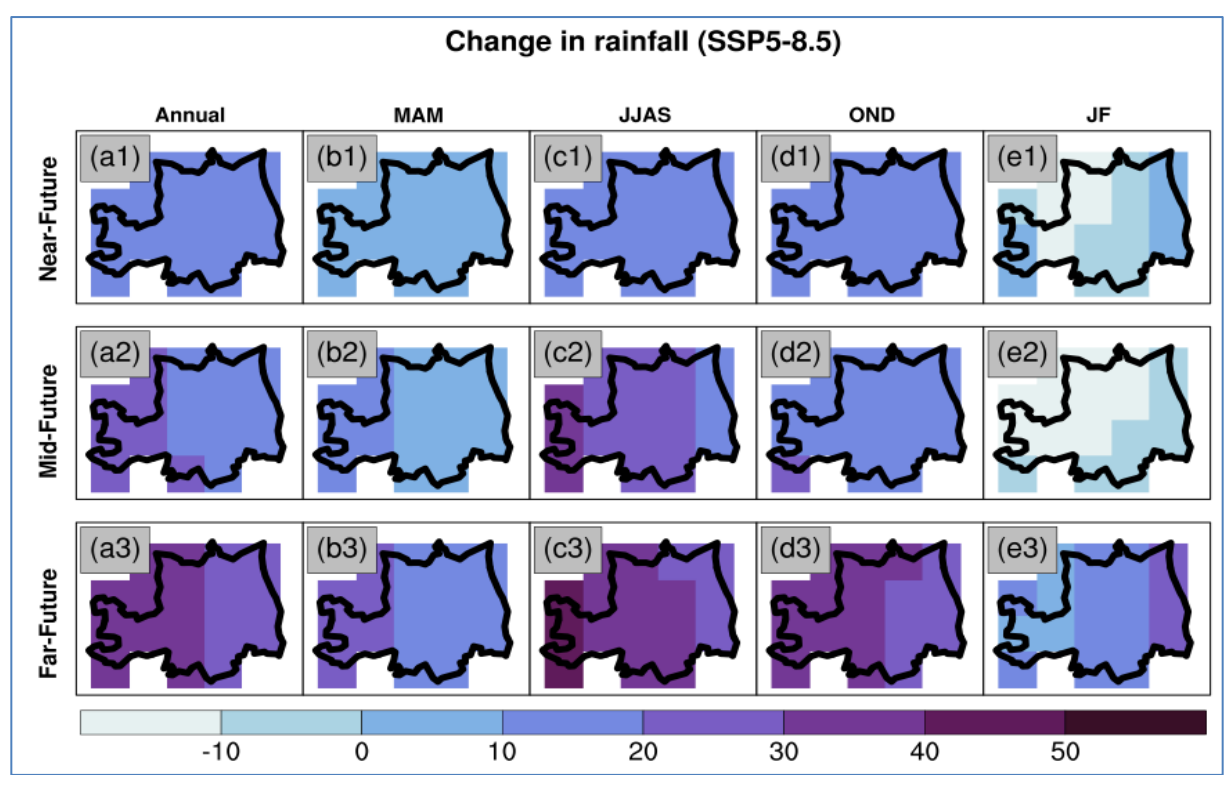
 $\label{eq:TABLES2} \textbf{Results from the Taylor diagram for individual models}$

S.no	Model Name	Correlation	STD	RMSE
1,	ACCESS-CM2	0.557	3.176	3.44
2.	ACCESS-ESM1-5	0.50	3.20	3.66
3.	BCC-CSM2-MR	0.53	3.33	3.61
4.	CanESM5	0.57	3.05	3.37
5.	CMCC-CM2-SR5	0.55	3.32	3.51
6.	CMCC-ESM2	0.55	3.18	3.46
7.	CNRM-CM6-1	0.46	3.33	3.85
8.	CNRM-ESM2-1	0.48	3.64	3.89
9.	EC-Earth3	0.47	3.35	3.82
10.	EC-Earth3-Veg-LR	0.44	3.65	4.04
11.	FGOALS-g3	0.53	3.17	3.54
12.	GFDL-CM4_gr2	0.54	3.20	3.53
13.	GFDL-CM4	0.54	3.29	3.56
14.	GFDL-ESM4	0.53	3.18	3.53
15.	HadGEM3	0.47	3.22	3.77
16.	INM-CM4-8	0.53	3.26	3.55
17.	INM-CM5-0	0.45	3.64	4.01
18.	IPSL-CM6A-LR	0.62	3.00	3.18
19.	KACE-1-0-G	0.41	2.88	3.84
20.	KIOST-ESM	0.50	3.16	3.65

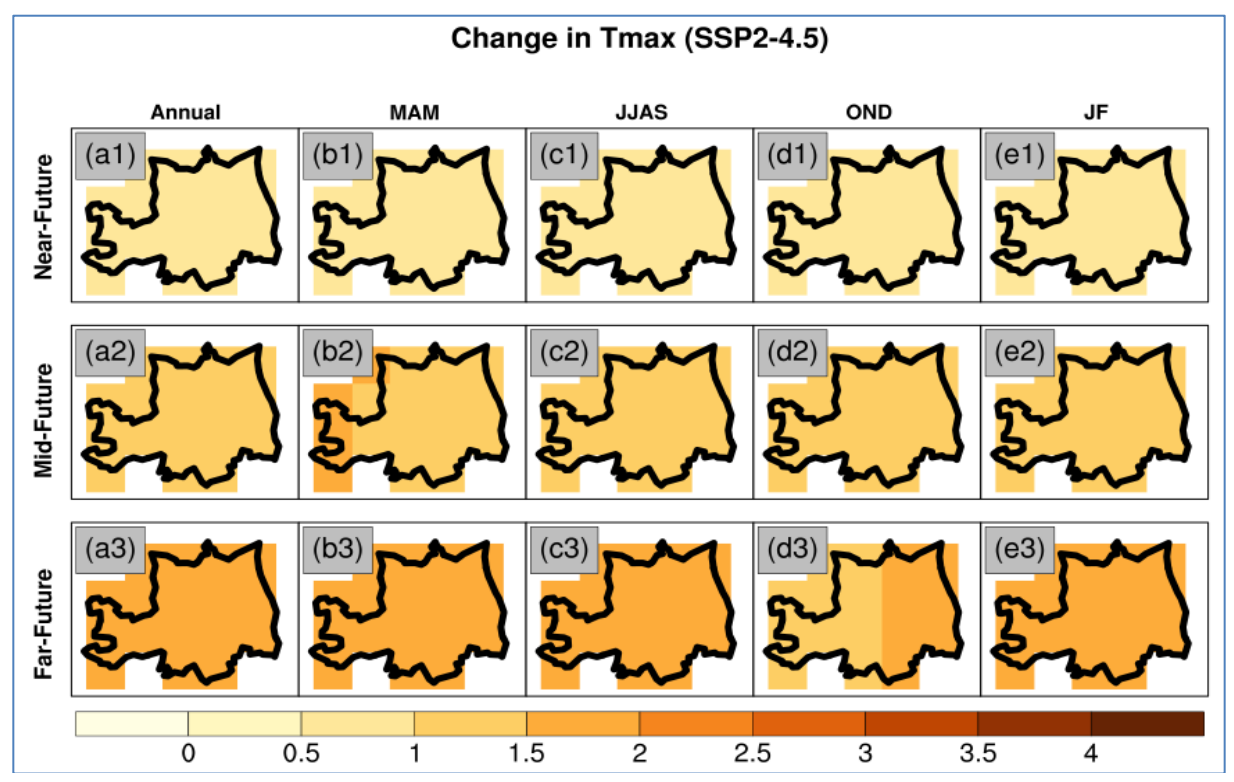
S.no	Model Name	Correlation	STD	RMSE
21.	MIROC6	0.53	3.33	3.58
22.	MIROC-ES2L	0.60	3.11	3.28
23.	MPI-ESM1-2-HR	0.48	3.09	3.69
24.	MPI-ESM1-2-LR	0.51	3.17	3.61
25.	MRI-ESM2-0	0.43	3.46	4.01
26.	NESM3	0.52	3.11	3.55
27.	NorESM2-LM	0.50	3.65	3.84
28.	NorESM2-MM	0.47	3.76	3.98
29.	UKESM1-0-LL	0.53	3.27	3.56



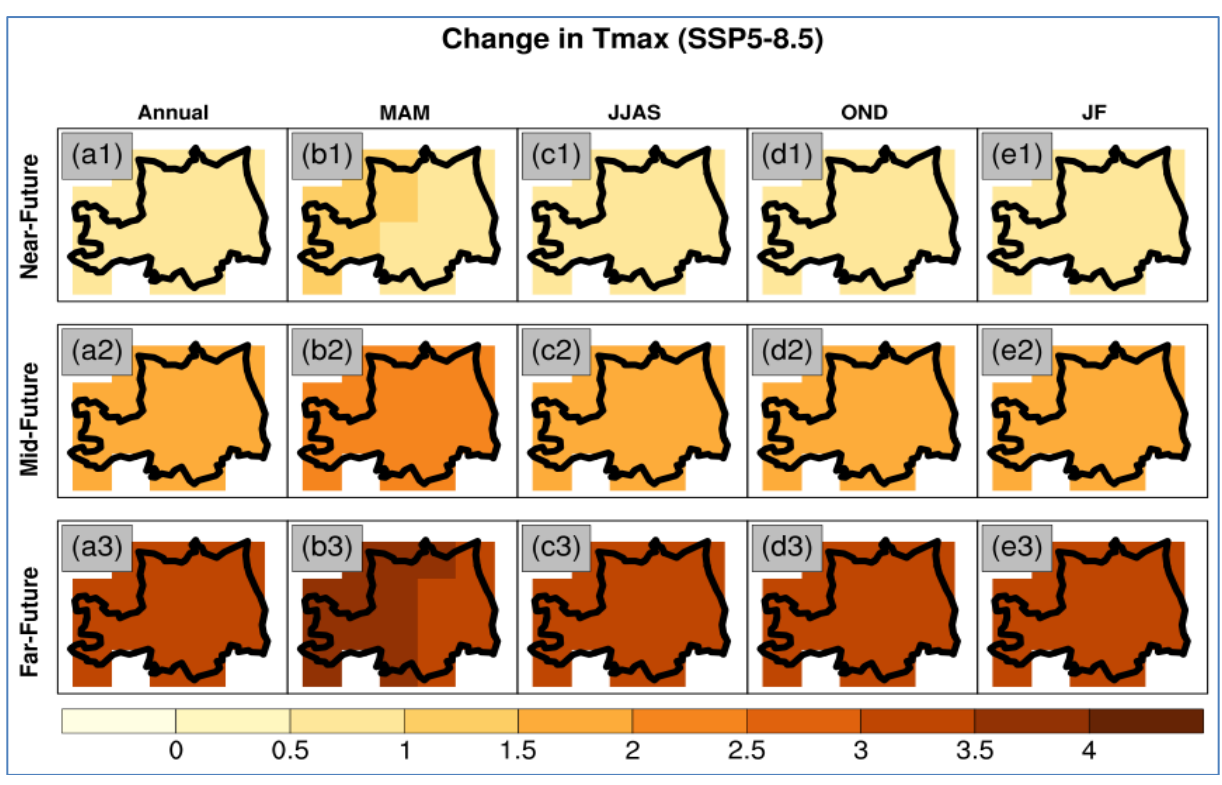
Figs. S3(a1-e3). Spatial heterogeneity of change in rainfall (%) in the future with respect to 1981-2010 over Tirupati district across seasons in SSP2-4.5



Figs. S4(a1-e3). Spatial heterogeneity of change in rainfall (%) in the future with respect to 1981-2010 over Tirupati district across seasons in SSP4-8.5



Figs. S5(a1-e3). Spatial heterogeneity of change in T_{max} (°C) in the future with respect to 1981-2010 over Tirupati district across seasons for SSP2-4.5



Figs. S6(a1-e3). Spatial heterogeneity of change in T_{max} (°C) in the future with respect to 1981-2010 over Tirupati district across seasons for SSP5-8.5

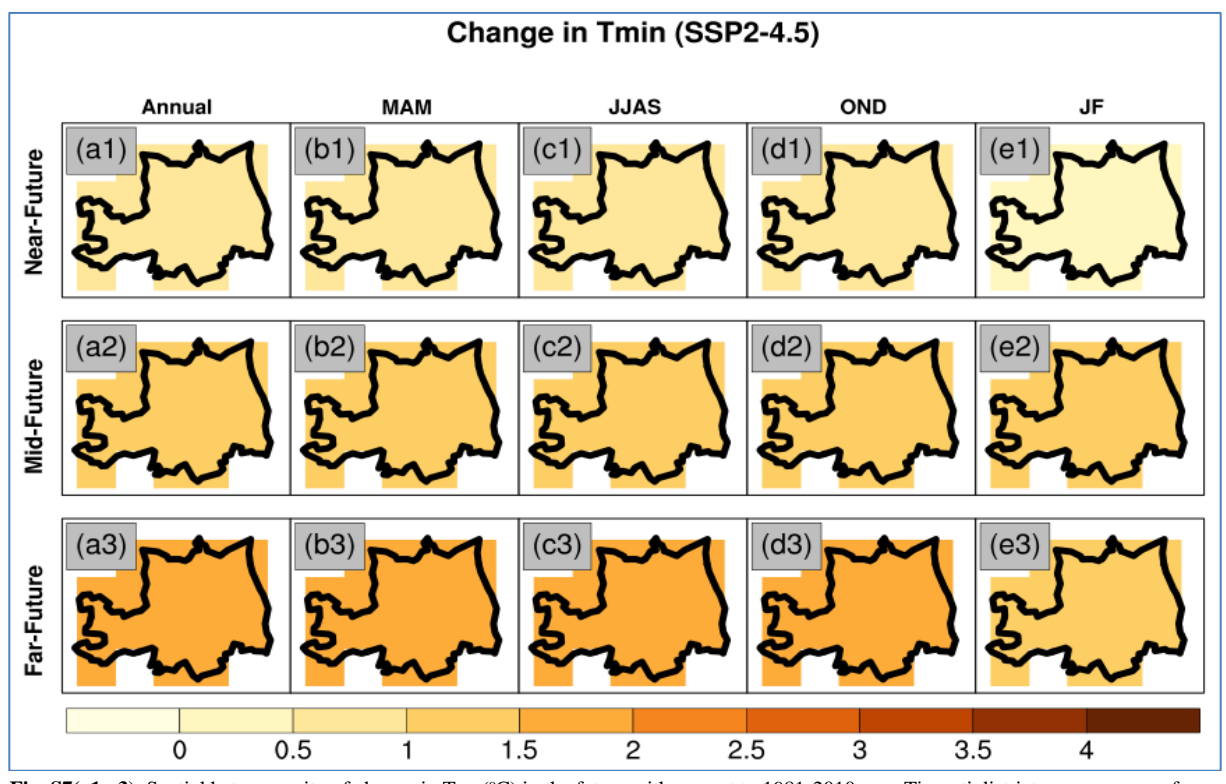


Fig. S7(a1-e3). Spatial heterogeneity of change in T_{min} (°C) in the future with respect to 1981-2010 over Tirupati district across seasons for SSP2-4.5

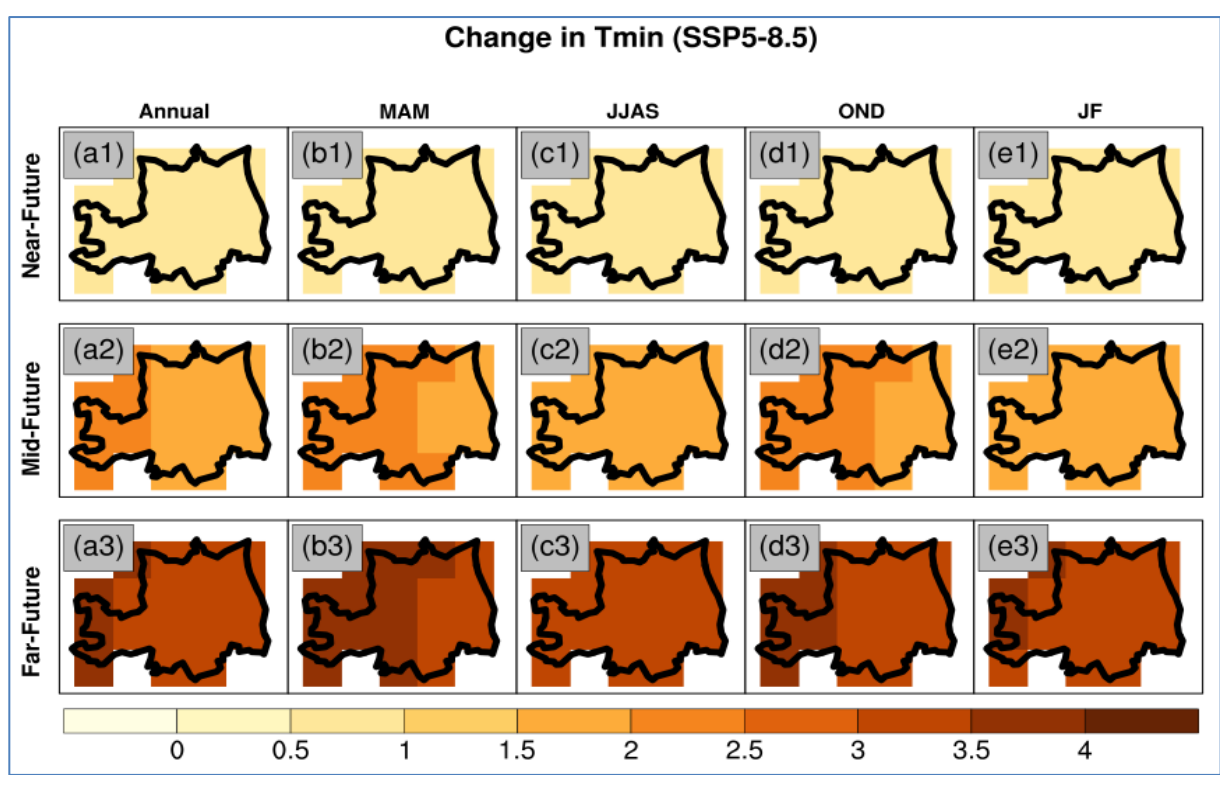


Fig. S8(a1-e3). Spatial heterogeneity of change in T_{min} (°C) in the future with respect to 1981-2010 over Tirupati district across seasons for SSP5-8.5

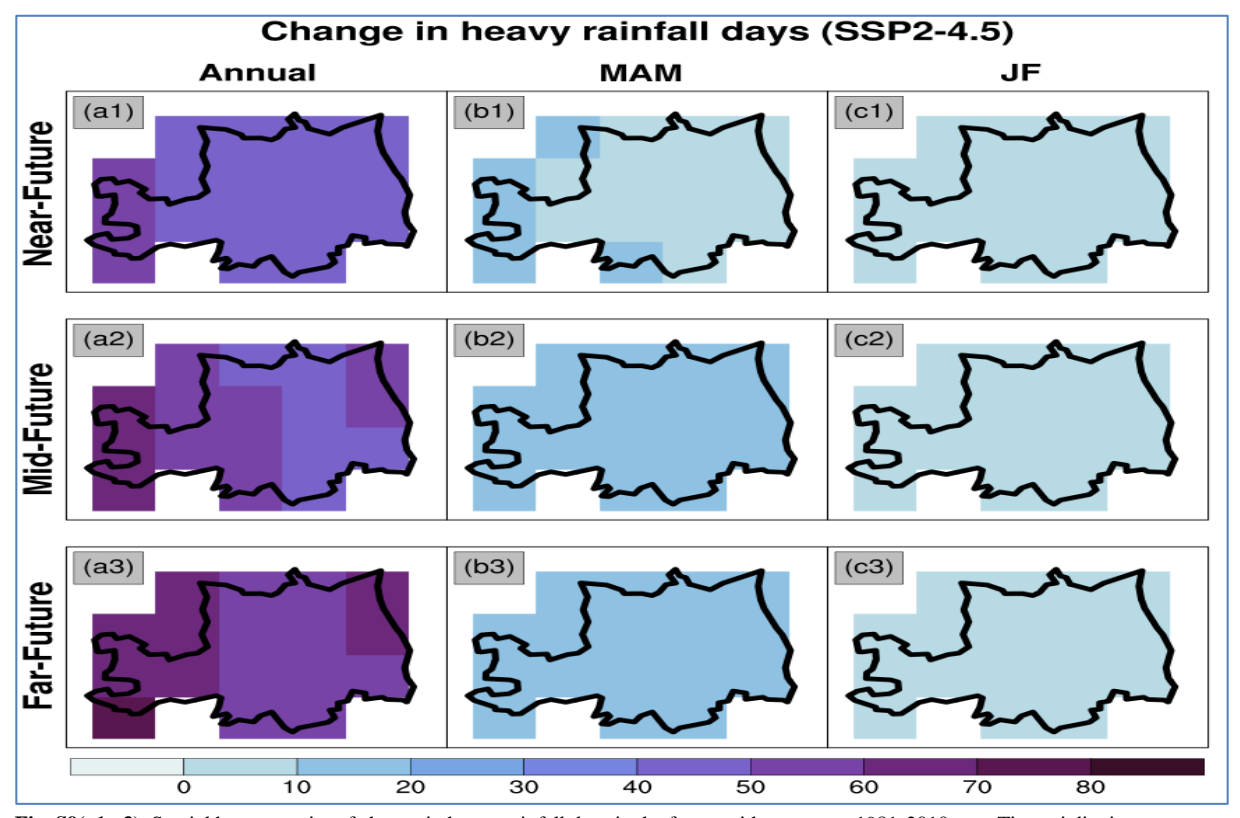
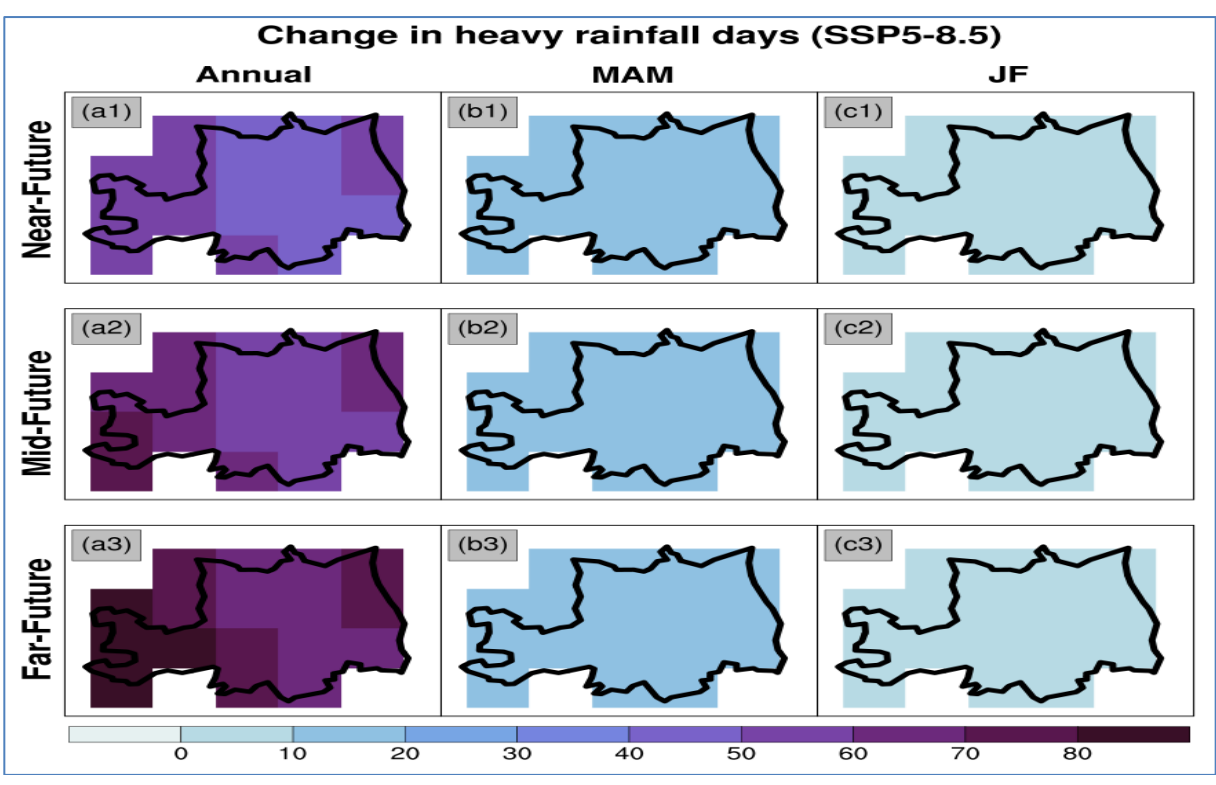
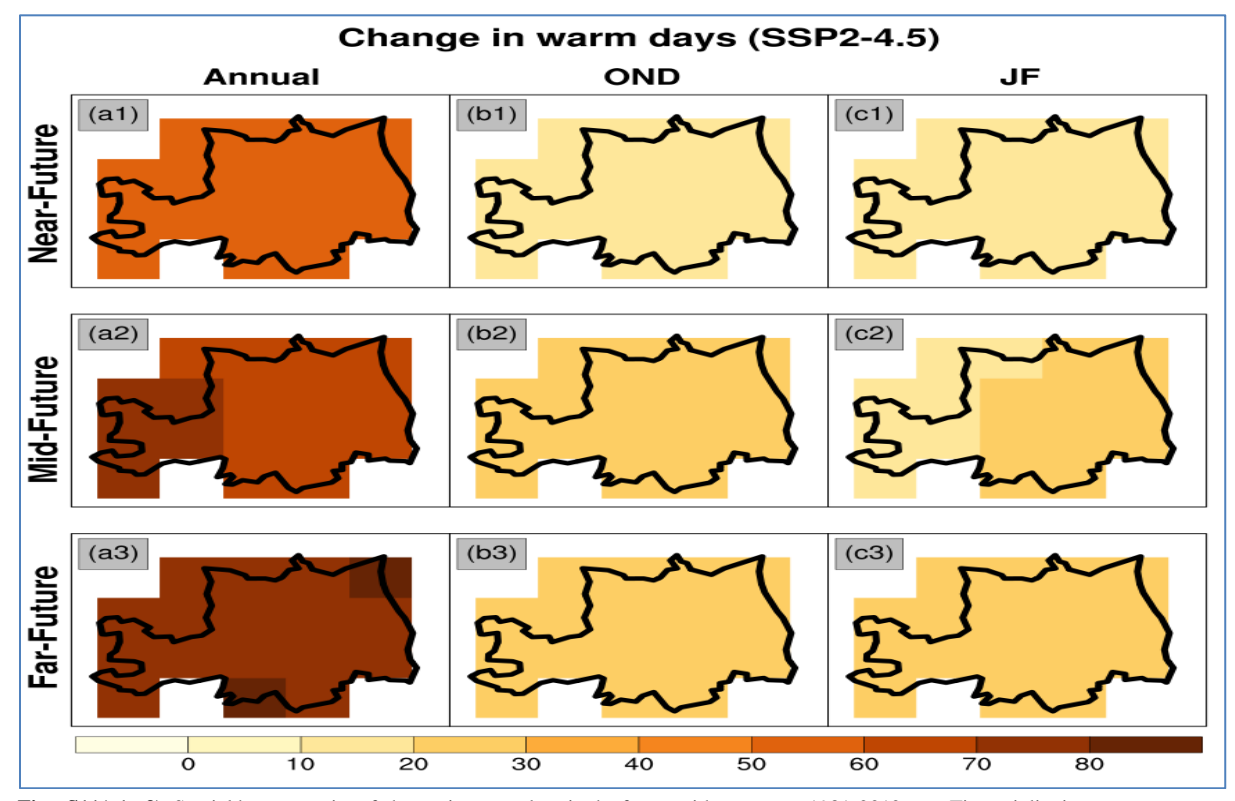


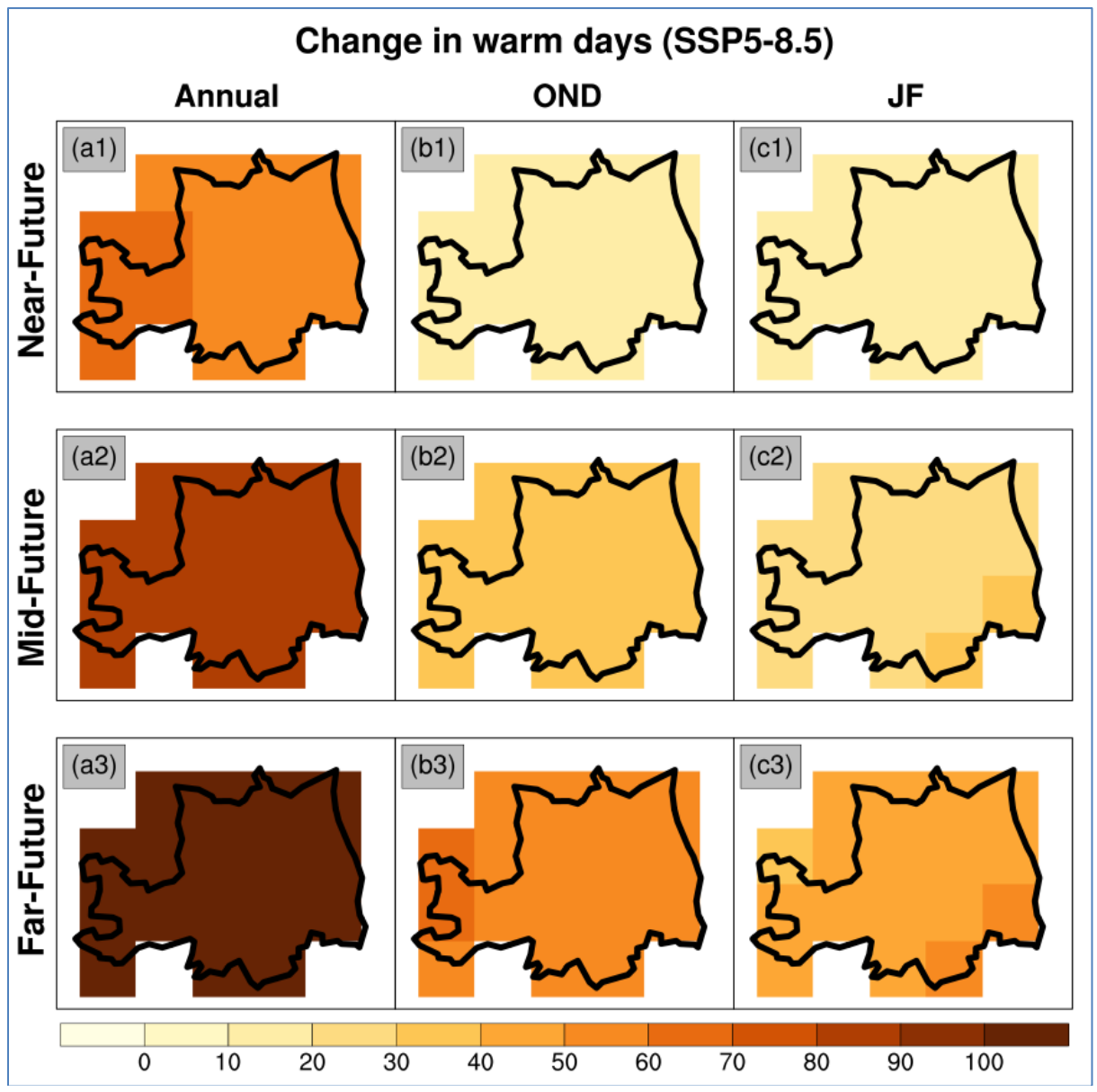
Fig. S9(a1-c3). Spatial heterogeneity of change in heavy rainfall days in the future with respect to 1981-2010 over Tirupati district across seasons for SSP2-4.5



Figs. S10(a1-c3). Spatial heterogeneity of change in heavy rainfall days in the future with respect to 1981-2010 over Tirupati district across seasons for SSP5-8.5



Figs. S11(a1-c3). Spatial heterogeneity of change in warm days in the future with respect to 1981-2010 over Tirupati district across seasons for SSP2-4.5



Figs. S12(a1-c3). Spatial heterogeneity of change in warm days in the future with respect to 1981-2010 over Tirupati district across seasons for SSP5-8 5

•